Experimental and Computational Approach of Understanding the Gas Adsorption in Amino Functionalized Interpenetrated Metal Organic Frameworks (MOFs)

(Supporting information contains 57 pages including this page)

Pradip Pachfule[a], Yifei Chen[b], Jianwen Jiang[b] and Rahul Banerjee[a]*

[a] *Physical/Materials Chemistry Division, National Chemical Laboratory, Dr. Homi Bhabha Road, Pune-411008, India.*

[b] *Department of Chemical and Biomolecular Engineering, National University of Singapore, 117576, Singapore.*

E-mail: r.banerjee@ncl.res.in Fax: + 91-20-25902636; Tel: + 91-20-25902535

Supporting Information

CONTENT

Section S1. Detailed synthetic procedures and PXRD patterns for Cd-ANIC-1 and Co-ANIC-1. **S-3**

Section S2. Single crystal X-ray diffraction data collection, structure solution and refinement procedures. **S-8**

Section S3. TGA data and the thermal stability of Cd-ANIC-1 and Co-ANIC-1. **S-20**

Section S4. Gas adsorption analysis of Cd-ANIC-1 and Co-ANIC-1. **S-22**

Section S5. Single crystal structures of Cd-ANIC-1 and Co-ANIC-1. **S-33**

Section S6. Computational Studies for Cd-ANIC-1 and Co-ANIC-1. **S-39**

Section S1. Detailed synthesis procedures MOFs including multi-gram scale products, experimental and simulated PXRD patterns:

2-amino-4-pyridylcarboxylic acid (2-amino-isonicotinic acid) was purchased from Alfa Aesar and $Cd(NO_3)_2.4H_2O$, $Co(NO_3)_2.6H_2O$ were purchased from Aldrich Chemicals. *N*, *N*-dimethylformamide (DMF) was purchased from Rankem chemicals. All starting materials were used without further purification. All experimental operations were performed in air and all the stock solutions were prepared in *N*, *N*-dimethylformamide (DMF).

Synthesis of [Cd(ANIC)$_2$] ($C_{12}H_{12}N_4O_4Cd$) (Cd-ANIC-1): A solution of $Cd(NO_3)_2{\cdot}4H_2O$ (37 mg, 0.12 mmol) and ANIC (69 mg, 0.50 mmol) in DMF/EtOH (6:1, 7 mL) was heated under controlled heating at 120 ºC for 2 days in a Teflon-lined steel bomb. The resulting colorless crystals were collected, washed with DMF, and dried at room temperature (yield: 19 mg, 54% based on Cd).

FT-IR: (KBr 4000-600 cm^{-1}): 3256(m, br), 2976(w), 2308(w), 1675(s), 1642(s), 1530(s), 1452(m), 1360(s), 1244(m), 774(m) cm^{-1}.

Elemental analysis (%) calcd: C 37.08, H 3.11, N 18.62; found: C 36.35, H 2.96, N 18.96.

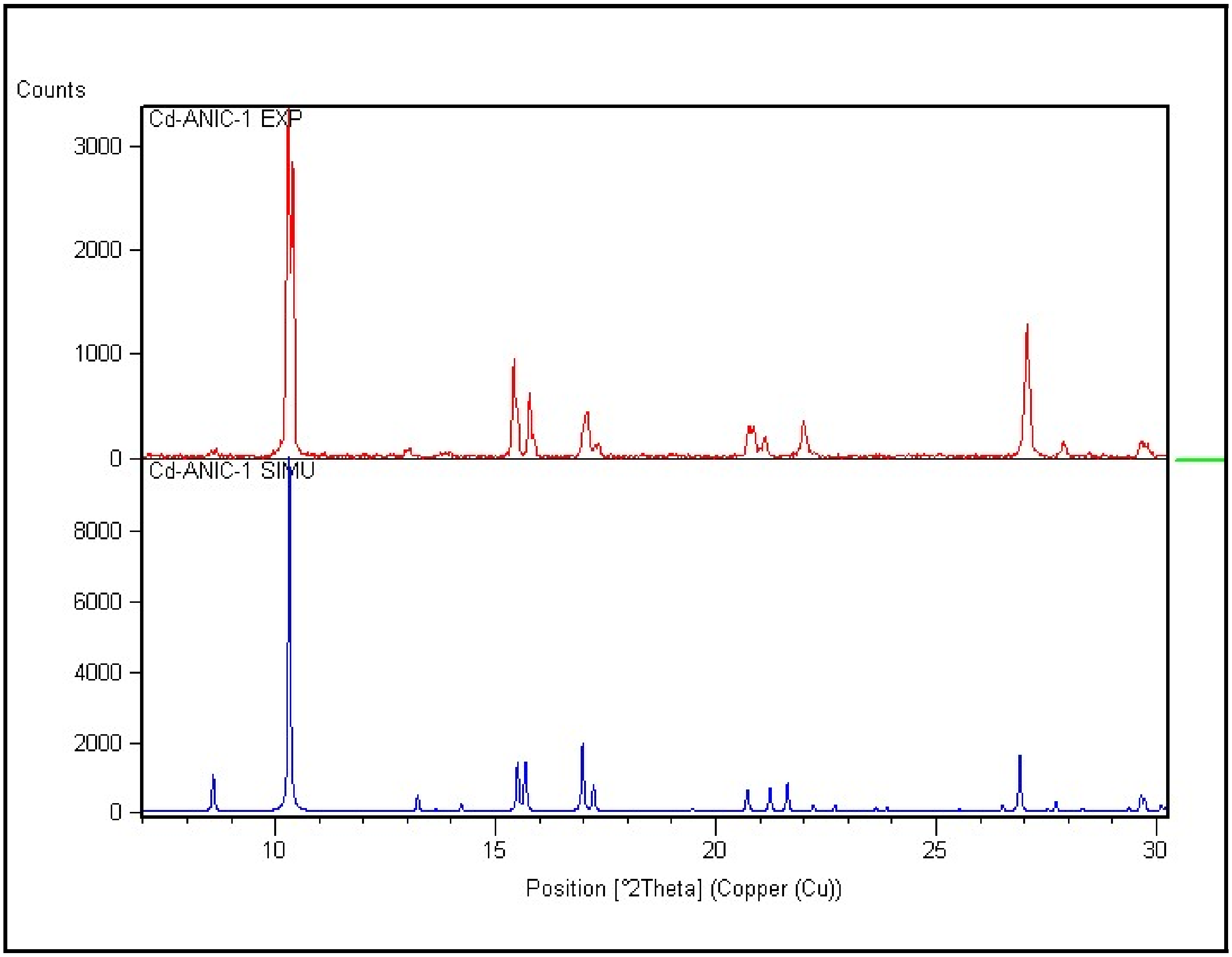

Figure S1. Comparison of the experimental PXRD pattern of as-synthesized Cd-ANIC-1 (top) with the one simulated from its single crystal structure (bottom).

Synthesis of [Co(ANIC)$_2$] ($C_{12}H_{12}N_4O_4Co$) Co-ANIC-1: A solution of $Co(NO_3)_2{\cdot}6H_2O$ (35 mg, 0.12 mmol) and ANIC (69 mg, 0.50 mmol) in DMF/EtOH (6:1, 7 mL) was heated under controlled heating at 120 ºC for 2 days in a Teflon-lined steel bomb. The resulting pink colored crystals were collected, washed with DMF, and dried at room temperature (yield: 17 mg, 48% based on Co).

FT-IR: (KBr 4000-600 cm^{-1}): 3258(m, br), 2977(w), 2311(w), 1682(s), 1586(s), 1534(s), 1454(m), 1371(s), 1243(m), 990(m), 808(m), 771(m) cm^{-1}.

Elemental analysis (%) calcd: C 43.25, H 3.02, N 16.80; found: C 42.63, H 2.99, N 17.04.

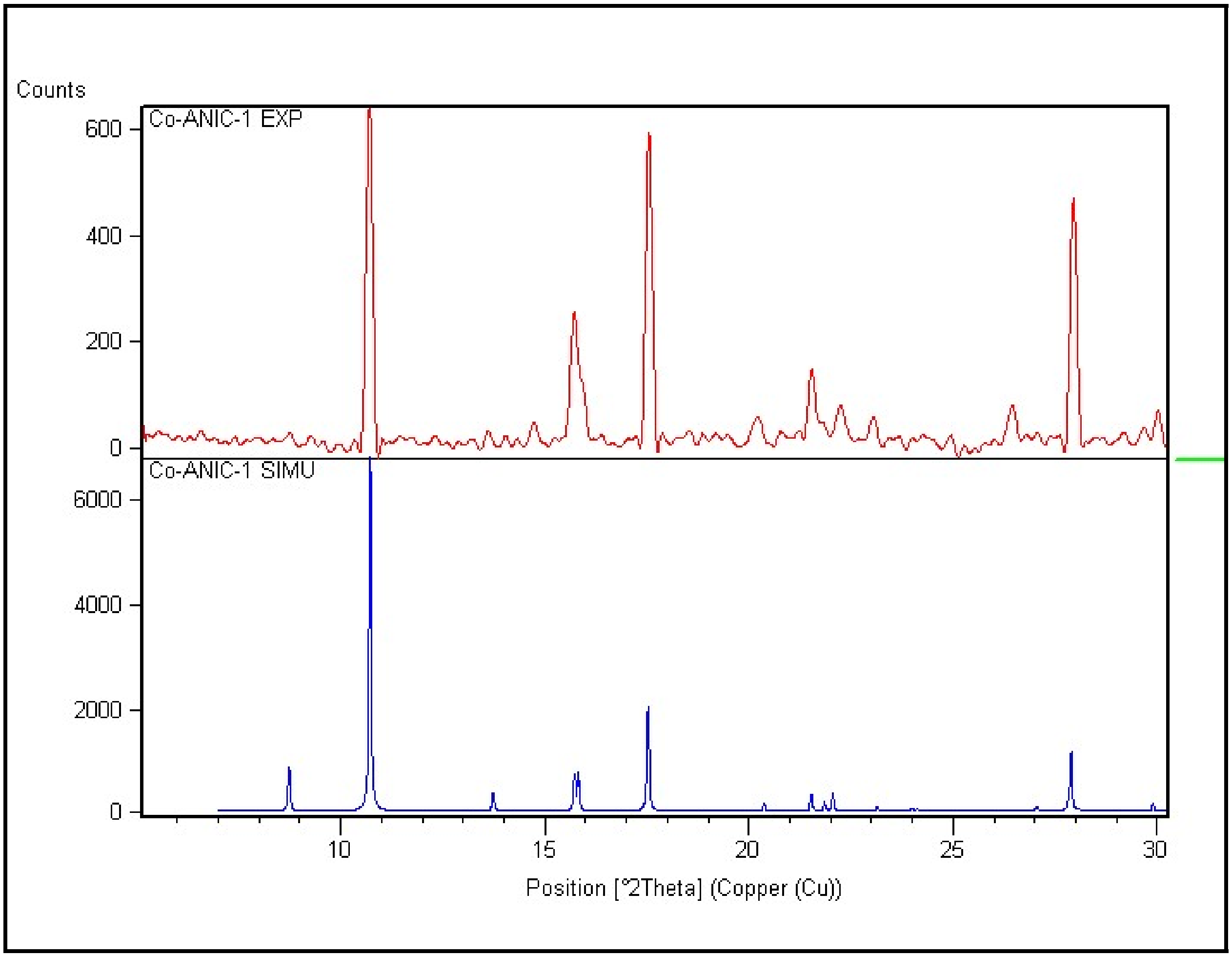

Figure S2. Comparison of the experimental PXRD pattern of as-synthesized Co-ANIC-1 (top) with the one simulated from its single crystal structure (bottom).

IR Absorption spectrums

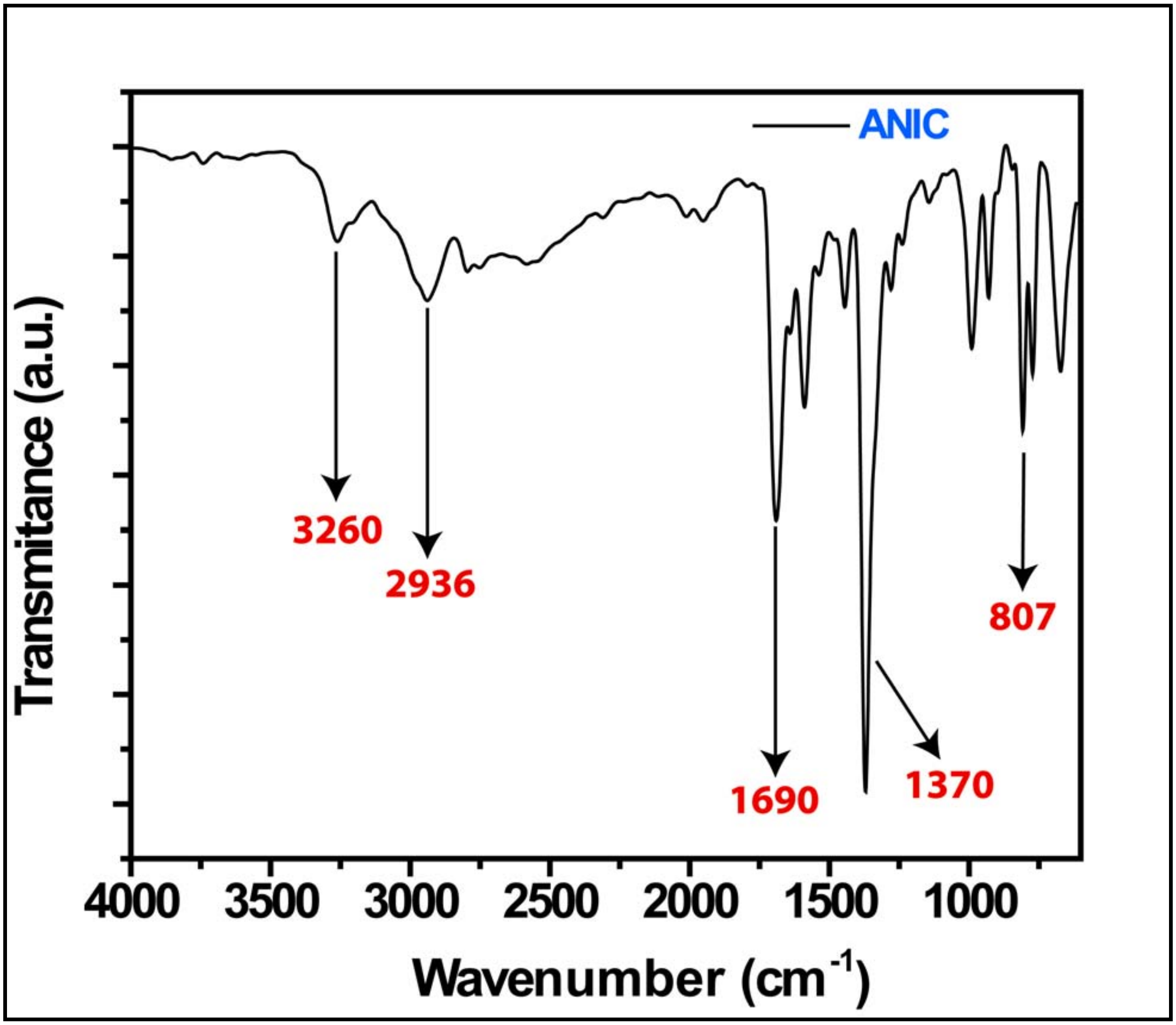

Figure S3. IR Absorption spectrum of 2-amino-isonicotinic acid (ANIC).

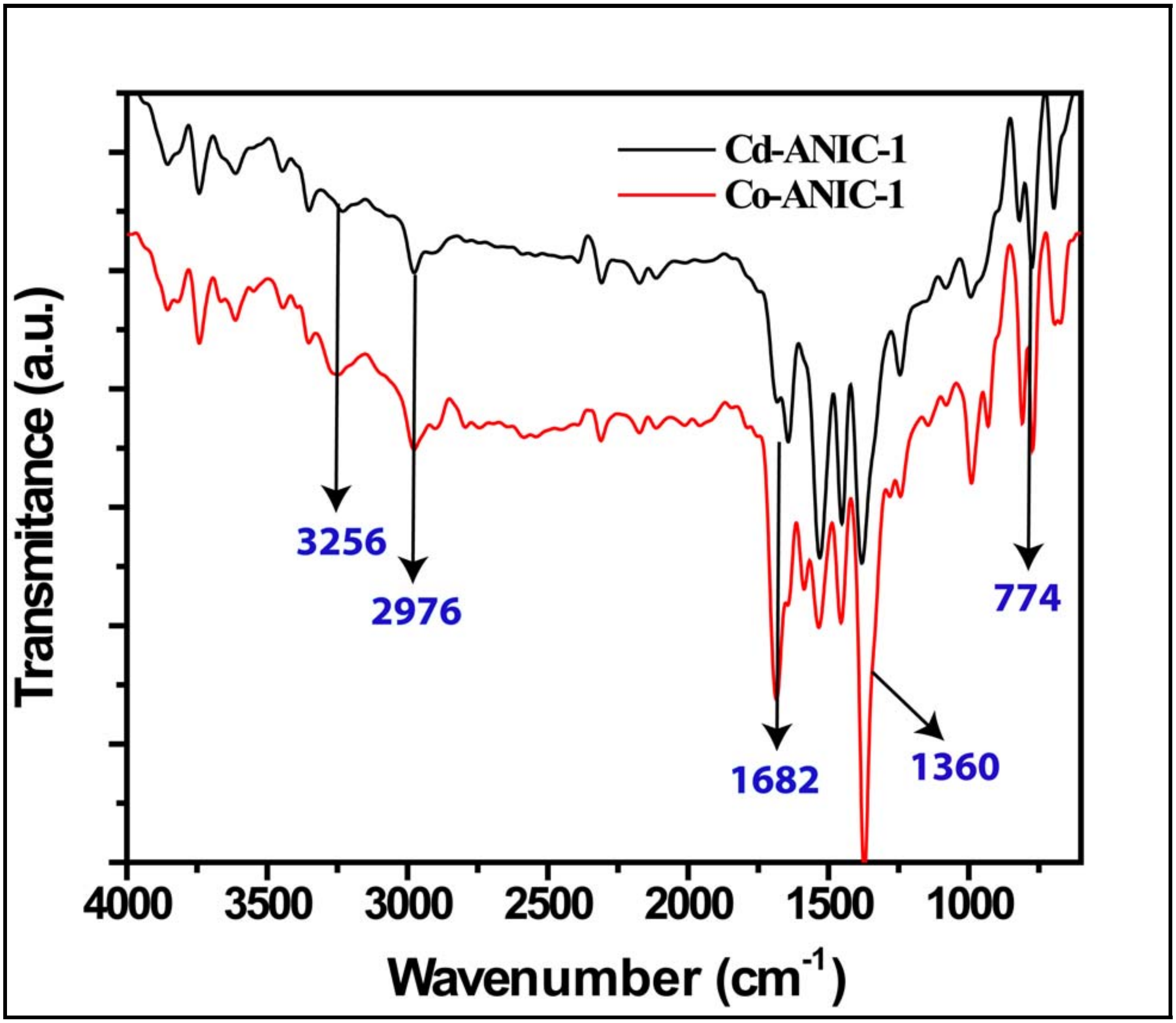

Figure S4. IR Absorption spectrums of Cd-ANIC-1 (black) and Co-ANIC-1 (red). IR stretching indicates the presence of uncoordinated –NH_2 functionality in the MOFs.

Section S2. Single crystal X-ray diffraction data collection, structure solution and refinement procedures:

General Data Collection and Refinement Procedures:

Single crystal data were collected on Bruker SMART APEX three circle diffractometer equipped with a CCD area detector and operated at 1500 W power (50 kV, 30 mA) to generate Mo K_α radiation (λ=0.71073 Å). The incident X-ray beam was focused and monochromated using Bruker Excalibur Gobel mirror optics. Crystals of all MOFs reported in the paper was mounted on nylon CryoLoop (Hampton Research) with Paraton-N (Hampton Research).

Initial scans of each specimen were performed to obtain preliminary unit cell parameters and to assess the mosaicity (breadth of spots between frames) of the crystal to select the required frame width for data collection. In every case frame widths of 0.5° were judged to be appropriate and full hemispheres of data were collected using the *Bruker SMART*[1] software suite. Following data collection, reflections were sampled from all regions of the Ewald sphere to redetermine unit cell parameters for data integration and to check for rotational twinning using *CELL_NOW*[2]. In no data collection was evidence for crystal decay encountered. Following exhaustive review of the collected frames the resolution of the dataset was judged. Data were integrated using Bruker *SAINT*[3] software with a narrow frame algorithm and a 0.400 fractional lower limit of average intensity. Data were subsequently corrected for absorption by the program *SADABS*[4]. The space group determinations and tests for merohedral twinning were carried out using *XPREP*[3]. In these cases, the highest possible space group was chosen.

Structures were solved by direct methods and refined using the *SHELXTL 97*[5] software suite. Atoms were located from iterative examination of difference F-maps following least squares refinements of the earlier models. Final model was refined anisotropically (if the number of data permitted) until full convergence was achieved. Hydrogen atoms were placed in calculated positions (C-H = 0.93 Å) and included as riding atoms with isotropic displacement parameters 1.2-1.5 times U_{eq} of the attached C atoms. In some cases modeling of electron density within the voids of the frameworks did not lead to identification of recognizable solvent molecules in these structures, probably due to the highly disordered contents of the large pores in the frameworks. Highly porous crystals that contain solvent-filled pores often yield raw data where observed strong (high intensity) scattering becomes limited to ~1.0 Å at best, with higher resolution data present at low intensity. A common strategy for improving X-ray data, increasing the exposure time of the crystal to X-rays, did not improve the quality of the high angle data in these cases, as the intensity from low angle data saturated the detector and minimal improvement in the high angle data was achieved. Additionally, diffuse scattering from the highly disordered solvent within the void spaces of the framework and from the capillary to mount the crystal contributes to the background and the 'washing out' of the weaker data. The only optimal crystals suitable for analysis were generally small and weakly diffracting. Unfortunately, larger crystals, which would usually improve the quality of the data, presented a lowered degree of crystallinity and attempts to optimize the crystal growing conditions for large high-quality specimens have not yet been fruitful. Single Crystal X-ray Diffraction data for Cd-ANIC-1 and Co-ANIC-1 was collected at 298(2) K. Electron density within void spaces has not been assigned to any guest entity but has been modeled as isolated oxygen and/or carbon atoms. The foremost errors in all the models are thought to lie in the assignment of guest electron density. Structures were examined using the *ADDSYM* subroutine of *PLATON*[7] to assure that no additional symmetry could be applied to the models. All ellipsoids in *ORTEP* diagrams are displayed at the

50% probability level unless noted otherwise. For these structures we noted that elevated R-values are commonly encountered in MOF crystallography for the reasons expressed above by some research groups.[8-17] Table S1 and S2 contains crystallographic data for the all MOFs. Crystallographic data (excluding structure factors) for the structures reported in this paper have been deposited with the CCDC as deposition No. CCDC 822054 - 822055. Copies of the data can be obtained, free of charge, on application to the CCDC, 12 Union Road, Cambridge CB2 lEZ UK (fax: + 44 (1223) 336 033; e-mail: deposit@ccdc.cam.ac.uk).

1. Bruker (2005). *APEX2*. Version 5.053. Bruker AXS Inc., Madison, Wisconsin, USA.
2. Sheldrick, G. M. (2004). *CELL_NOW*. University of Göttingen, Germany. Steiner, Th. (1998). *Acta Cryst*. B54, 456–463.
3. Bruker (2004). *SAINT-Plus* (Version 7.03). Bruker AXS Inc., Madison, Wisconsin, USA.
4. Sheldrick, G. M. (2002). *SADABS* (Version 2.03) and *TWINABS* (Version 1.02).University of Göttingen, Germany.
5. Sheldrick, G. M. (1997). *SHELXS '97* and *SHELXL '97*. University of Göttingen, Germany.
6. WINGX
7. A. L. Spek (2005) PLATON, *A Multipurpose Crystallographic Tool*, Utrecht University, Utrecht, The Netherlands.
8. Dakin, L. A., Ong P. C., Panek, J. S., Staples, R. J. & Stavropoulos, P. *Organometallics* **19**, 2896-2908 (2000).
9. Noro, S., Kitaura, R., Kondo, M., Kitagawa, S., Ishii, T., Matsuzaka, H. & Yamashita, M. *J. Am. Chem. Soc.* **124**, 2568-2583 (2002).

10. Eddaoudi, M., Kim, J., Vodak, D., Sudik, A., Wachter, J., O'Keeffe, M. & Yaghi, O. M. *Proc. Natl. Acad. Sci. U.S.A.* **99**, 4900-4904 (2002).
11. Heintz, R. A., Zhao, H., Ouyang, X., Grandinetti, G., Cowen, J. & Dunbar, K. R. *Inorg. Chem.* **38**, 144-156 (1999).
12. Biradha, K., Hongo, Y. & Fujita, M. *Angew. Chem. Int. Ed.* **39**, 3843-3845 (2000).
13. Grosshans, P., Jouaiti, A., Hosseini, M. W. & Kyritsakas, N. *New J. Chem, (Nouv. J. Chim,)* **27**, 793-797 (2003).
14. Takeda, N., Umemoto, K., Yamaguchi, K. & Fujita, M. *Nature (London)* **398**, 794-796 (1999).
15. Eddaoudi, M., Kim, J., Rosi, N., Vodak, D., Wachter, J., O'Keeffe, M. & Yaghi, O. M. *Science* **295**, 469-472 (2002).
16. Kesanli, B., Cui, Y., Smith, M. R., Bittner, E. W., Bockrath, B. C. & Lin, W. *Angew. Chem. Int. Ed.* **44,** 72-75 (2005).
17. Cotton, F. A., Lin, C. & Murillo, C. A. *Inorg. Chem.* **40**, 478-484 (2001).

Cd-ANIC-1 (Orthorhombic)

Experimental and Refinement Details for Cd-ANIC-1:

A colorless plate type crystal (0.30 × 0.24 × 0.16 mm^3) of Cd-ANIC-1 was mounted on 0.7 mm diameter nylon CryoLoops (Hampton Research) with Paraton-N (Hampton Research). The loop was mounted on a *SMART APEX* three circle diffractometer equipped with a CCD area detector (Bruker Systems Inc., 1999a)[19] and operated at 1500 W power (50 kV, 30 mA) to generate Mo K_α radiation (λ=0.71073 Å). The incident X-ray beam was focused and monochromated using Bruker Excalibur Gobel mirror optics. A total of 5973 reflections were collected of which 2296 were unique and 2076 of these were greater than 2σ (*I*). The range of θ was from 1.98 to 28.24°. Analysis of the data showed negligible decay during collection. The structure was solved in the tetragonal *Fddd* space group, with *Z* = 16, using direct methods. All the atoms were refined anisotropically with hydrogen atoms generated as spheres riding the coordinates of their parent atoms. Modeling of electron density within the voids of the frameworks did not lead to identification of solvent molecules in all structures due to the lowered resolution of the data. The attempts made to model the solvent molecules did not lead to identification it in all structures due to the limited periodicity of the solvent molecules in the crystals. Since the solvent is free in the framework this can be expected for the MOF structures. However, very high displacement parameters, high esd's and partial occupancy due to the disorder make it impossible to determine accurate positions for these solvent molecules. Thus, electron density within void spaces which could not be assigned to any definite guest entity was modeled as isolated carbon and oxygen atoms, and the foremost errors in all the models lies with assignment of guest electron density. To prove the correctness of the atomic positions in the framework the application of the

SQUEEZE routine of A. Spek has been performed. The unit cell of Cd-ANIC-1 contains 2 units of ANIC and per cadmium ion. Final full matrix least-squares refinement on $F2$ converged to $R_1 = 0.0659$ ($F > 2\sigma F$)) and $wR_2 = 0.1822$ (all data) with GOF = 1.340. It should be noted that other supporting characterization data (*vide infra* Section S1) are consistent with the crystal structure.

Table S1. **Crystal data and structure refinement for Cd-ANIC-1:**

Empirical formula	C12 H12 Cd N4 O4
Formula weight	388.67
Temperature	298(2) K
Wavelength	0.71073
Crystal system	Orthorhombic
Space group	*Fddd*
	a = 12.869(5) Å α = 90°
Unit cell dimensions	*b* = 23.643(10) Å β = 90°
	c = 24.900(11) Å γ = 90°
Volume	7576(5)
Z	16
Density (calculated)	1.363
Absorption coefficient	1.192
F(000)	3864
Crystal size	0.30 × 0.24 × 0.16 mm^3
Theta range for data collection	2.37 – 28.22
Index ranges	-17= h <= 16,-30<= k <= 30,-32<= l <= 32
Reflections collected	3864
Independent reflections	2076
Completeness to theta = 26.02°	97.7 %
Absorption correction	Semi-empirical from equivalents
Refinement method	Full-matrix least-squares on F^2
Data / restraints / parameters	2296/0/100
Goodness-of-fit on F^2	1.340
Final R indices [I>2sigma(I)]	R_1 = 0.0659, wR_2 = 0.1822
R indices (all data)	R_1 = 0.0688, wR_2 = 0.1853
Largest diff. peak and hole	0.265 and – 1.385 eÅ^{-3}

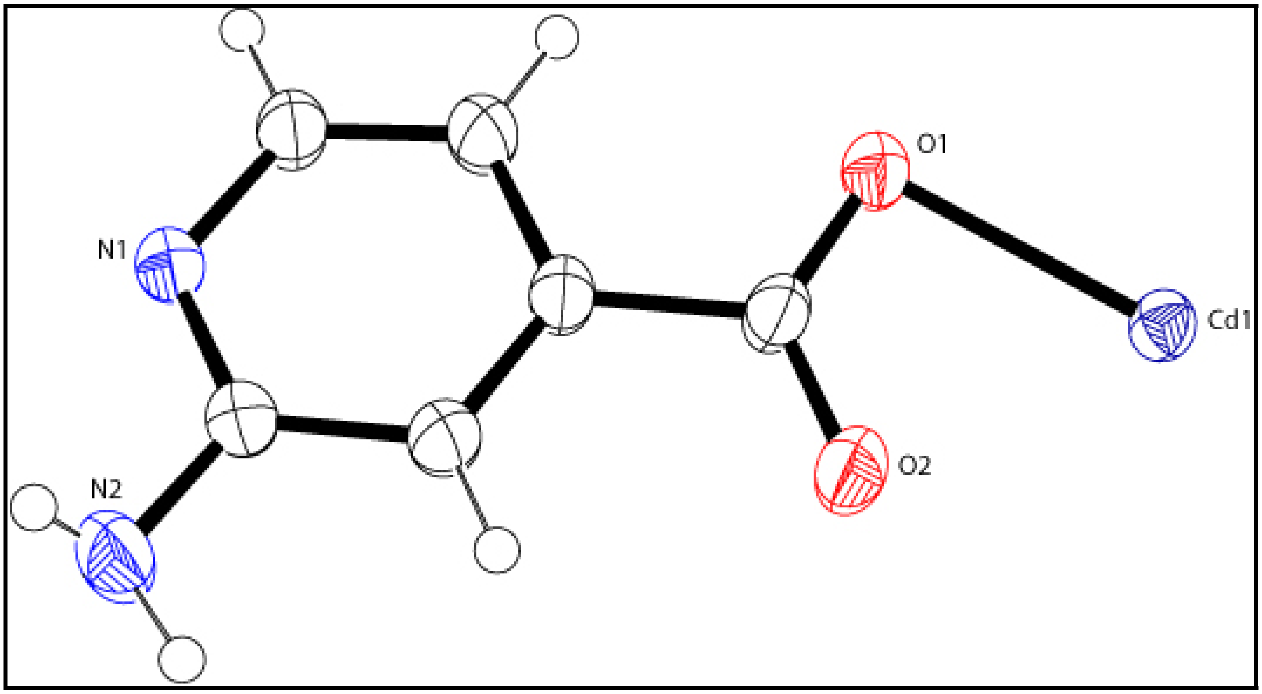

Figure S5. ORTEP drawing of the asymmetric unit of Cd-ANIC-1.

Co-ANIC-1 (Orthorhombic)

Experimental and Refinement Details for Co-ANIC-1:

A pink plate type crystal (0.24 × 0.15 × 0.12 mm^3) of Co-ANIC-1 was mounted on 0.7 mm diameter nylon CryoLoops (Hampton Research) with Paraton-N (Hampton Research). The loop was mounted on a *SMART APEX* three circle diffractometer equipped with a CCD area detector (Bruker Systems Inc., 1999a)[19] and operated at 1500 W power (50 kV, 30 mA) to generate Mo K_{α} radiation (λ=0.71073 Å). The incident X-ray beam was focused and monochromated using Bruker Excalibur Gobel mirror optics. A total of 3453 reflections were collected of which 2073 were unique and 1577 of these were greater than $2\sigma(I)$. The range of θ was from 2.01 to 28.26º. Analysis of the data showed negligible decay during collection. The structure was solved in the tetragonal *Fddd* space group, with $Z = 16$, using direct methods. All the atoms were refined anisotropically with hydrogen atoms generated as spheres riding the coordinates of their parent atoms. Modeling of electron density within the voids of the frameworks did not lead to identification of solvent molecules in all structures due to the lowered resolution of the data. The attempts made to model the solvent molecules did not lead to identification it in all structures due to the limited periodicity of the solvent molecules in the crystals. Since the solvent is free in the framework this can be expected for the MOF structures. However, very high displacement parameters, high esd's and partial occupancy due to the disorder make it impossible to determine accurate positions for these solvent molecules. Thus, electron density within void spaces which could not be assigned to any definite guest entity was modeled as isolated carbon and oxygen atoms, and the foremost errors in all the models lies with assignment of guest electron density. To prove the correctness of the atomic positions in the framework the application of the

SQUEEZE routine of A. Spek has been performed. The unit cell of Co-ANIC-1 contains 2 units of ANIC and per cobalt ion. Final full matrix least-squares refinement on $F2$ converged to $R_1 = 0.0335$ ($F > 2\sigma F$)) and $wR_2 = 0.1087$ (all data) with GOF = 1.110. It should be noted that other supporting characterization data (*vide infra* Section S1) are consistent with the crystal structure.

Table S2. Crystal data and structure refinement for Co-ANIC-1:

Empirical formula	C12 H10 Co N4 O4
Formula weight	333.17
Temperature	298(2) K
Wavelength	0.71073
Crystal system	Orthorhombic
Space group	*Fddd*
	$a = 12.819(2)$ Å $\alpha = 90°$
Unit cell dimensions	$b = 23.058(4)$ Å $\beta = 90°$
	$c = 23.654(4)$ Å $\gamma = 90°$
Volume	6992(2)
Z	16
Density (calculated)	1.266
Absorption coefficient	0.998
F(000)	2704
Crystal size	$0.24 \times 0.15 \times 0.12$ mm^3
Theta range for data collection	2.47 – 23.24
Index ranges	-16= h <= 16,-30<= k <= 30,-31<= l <= 30
Reflections collected	2704
Independent reflections	1577
Completeness to theta = 26.02°	95.7 %
Absorption correction	Semi-empirical from equivalents
Refinement method	Full-matrix least-squares on F^2
Data / restraints / parameters	2073/1/96
Goodness-of-fit on F^2	1.110
Final R indices [I>2sigma(I)]	$R_1 = 0.0335$, $wR_2 = 0.1087$
R indices (all data)	$R_1 = 0.0437$, $wR_2 = 0.1108$
Largest diff. peak and hole	0.071 and – 0.452 $eÅ^{-3}$

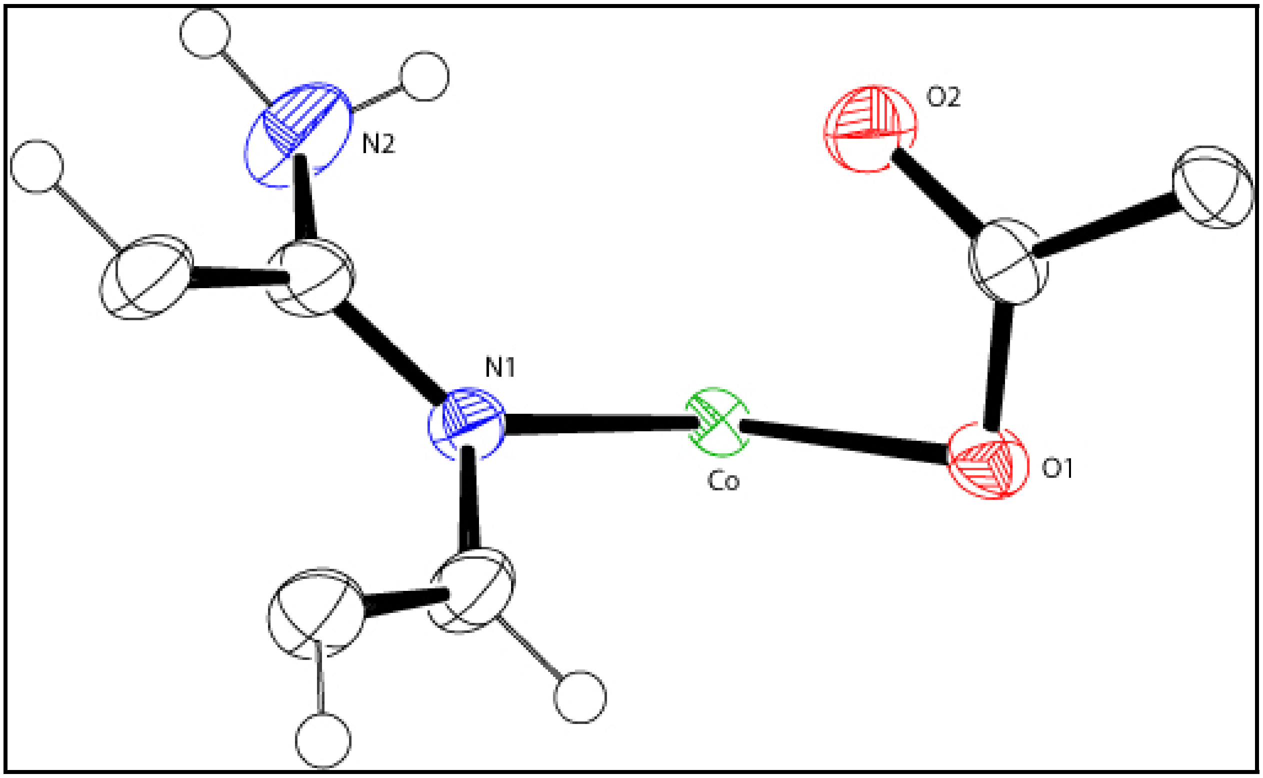

Figure S6. ORTEP drawing of the asymmetric unit of Co-ANIC-1.

Section S3. TGA data and the thermal stability of MOFs:

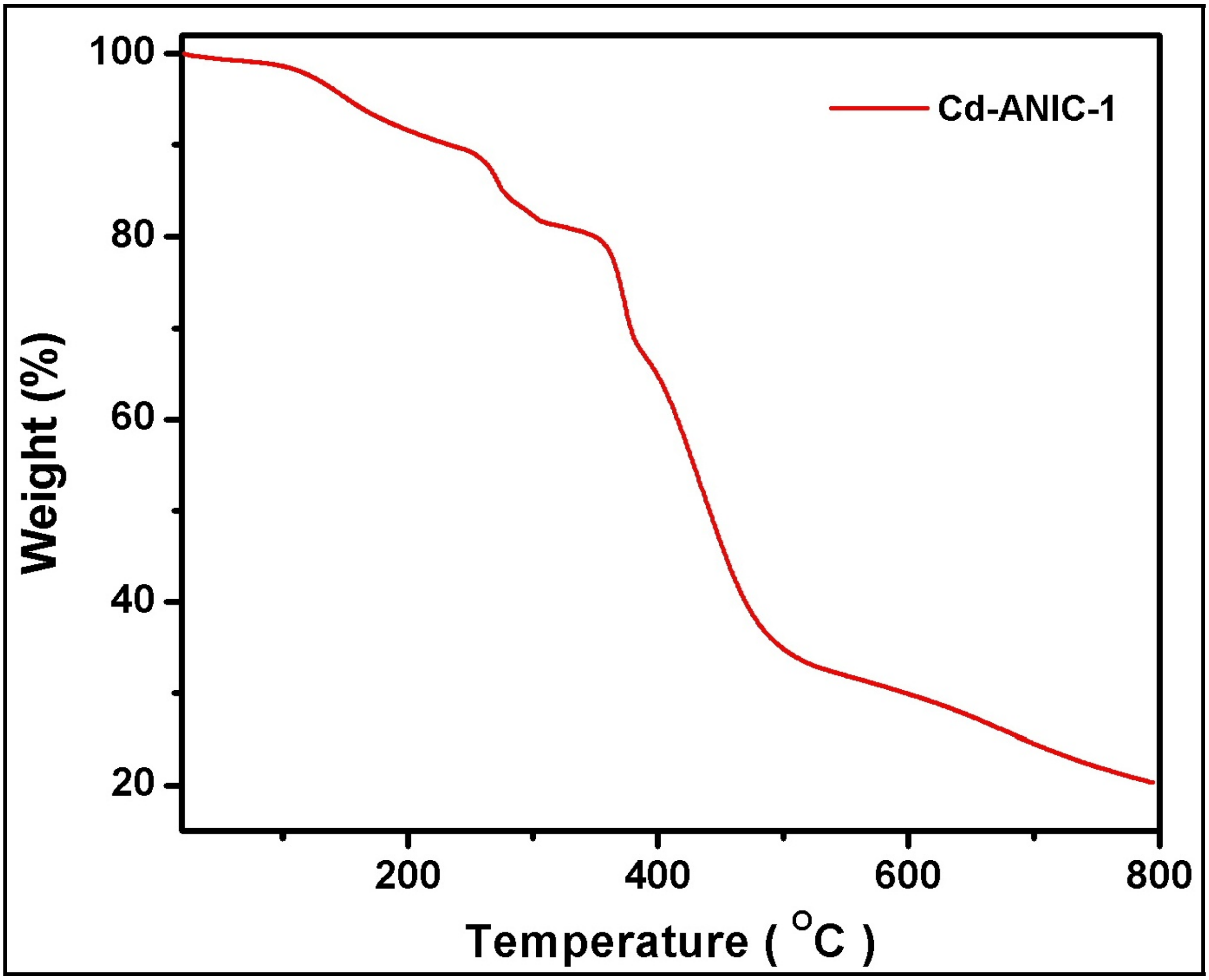

Figure S7. Thermal stability and the thermal gravimetric analysis (TGA) data of Cd-ANIC-1.

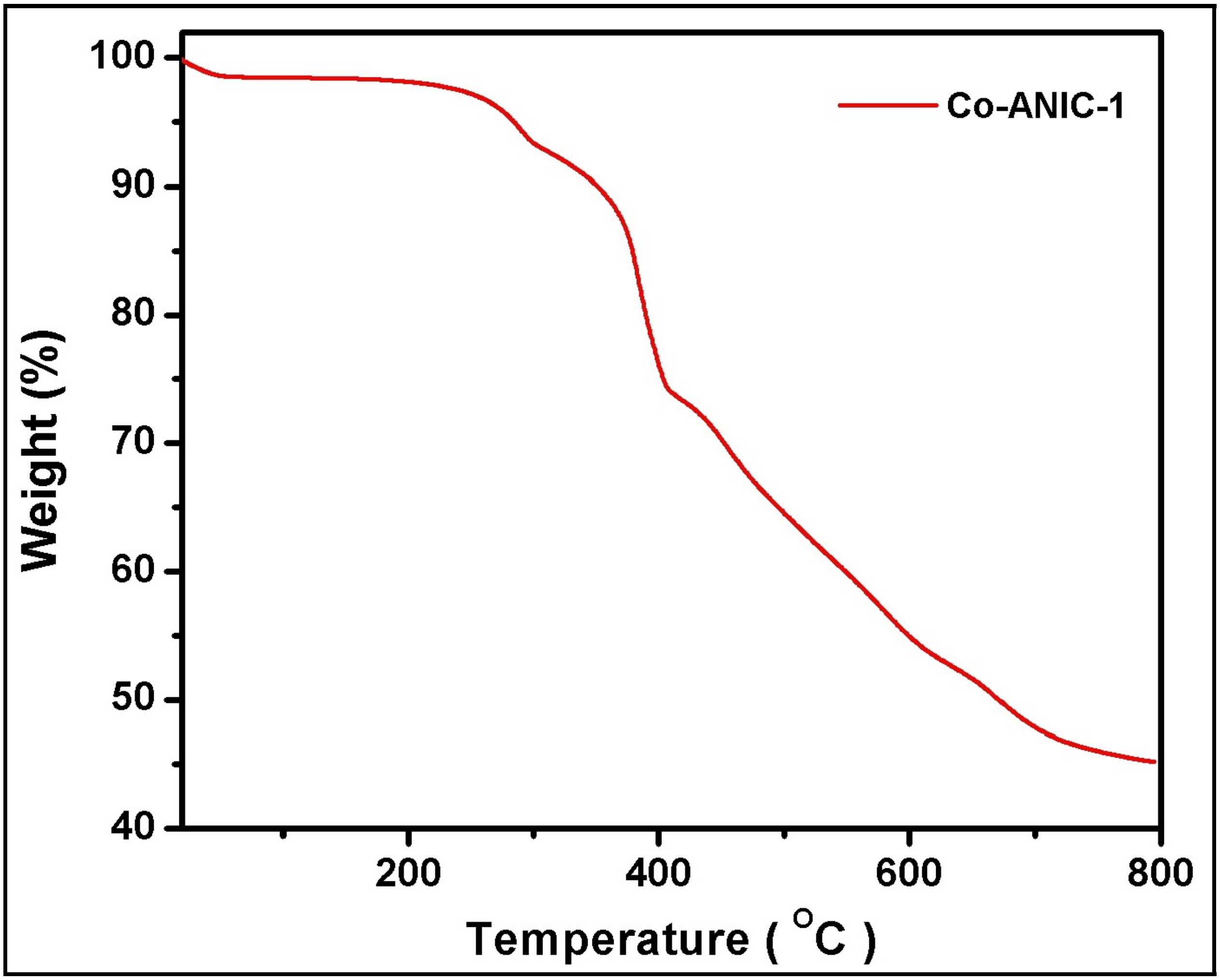

Figure S8. Thermal stability and the thermal gravimetric analysis (TGA) data of Co-ANIC-1.

Section S4. Gas adsorption analysis of Cd-ANIC-1 and Co-ANIC-1:

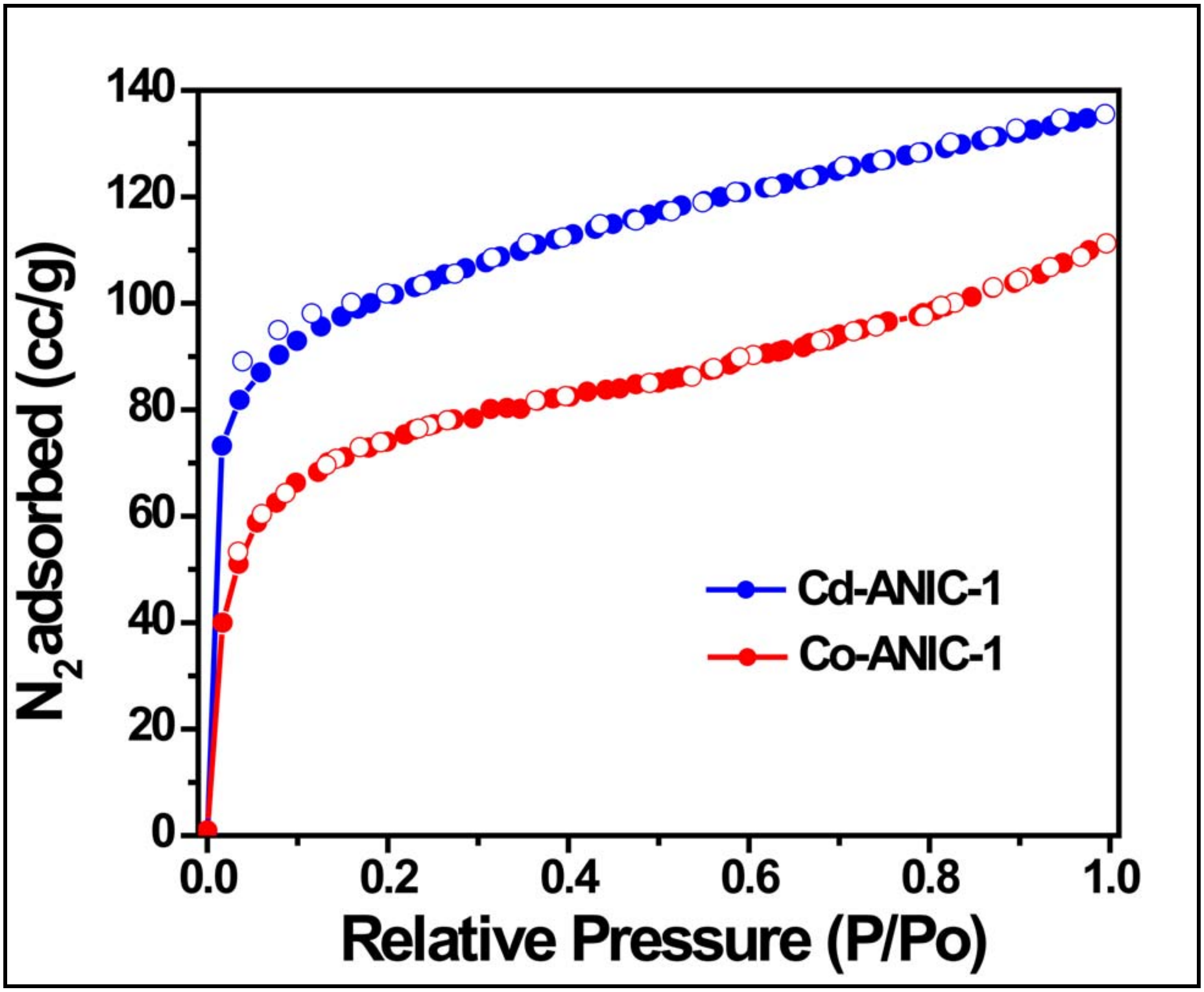

Figure S9. Typical Type-I Nitrogen adsorption isotherms for Cd-ANIC-1 and Co-ANIC-1 at 77 K and 1 atm pressure showing a Langmuir surface area of 504.95 and 412.65 m^2/g and BET surface area of 329.3 and 274.02 m^2/g, respectively.

Table S3. Comparison of Simultaneous H_2 and CO_2 adsorption capacity in same MOF**:

SL. No.**	Name of MOFs	H_2 uptake wt % at 1bar 77K	CO_2 uptake mmol/g at 1 bar		Reference
			273K	298K	
1	Ni\DOBDC	2.10	NA	5.8	S. R. Caskey, A. G. Wong-Foy, A. J. Matzger, *J. Am. Chem. Soc.* **2008**, *130*, 10870.
2	HKUST-1	2.54	NA	4.7	Q. M. Wang, D. Shen, M. Bulow, M. L. Lau, S. Deng, F.R. Fitch, N. O. Lemcoff, J. Semanscin, *Microporous and Mesoporous Materials*. **2002**, *55*, 217.
3	Mg\DOBDC	1.98	NA	8.08	S. R. Caskey, A. G. Wong-Foy, A. J. Matzger, *J. Am. Chem. Soc.* **2008**, *130*, 10870.
4	UTSA-20	2.80	NA	5.01	Z. Guo, H. Wu, G. Srinivas, Y. Zhou, S. Xiang, Z. Chen, Y. Yang, W. Zhou, M. O'Keeffe, B. Chen, *Angew. Chem. Int. Ed.* **2011**, *50*, 3178.
5	Cd-ANIC-1	1.84	4.72	3.84	This work
6	Co\DOBDC	1.81	NA	7.1	S. R. Caskey, A. G. Wong-Foy, A. J. Matzger, *J. Am. Chem. Soc.* **2008**, *130*, 10870.
7	CUK-1	1.60	NA	3.48	J. W. Yoon, S. H. Jhung, Y. K. Hwang, S. M. Humphrey, P. T. Wood, J. S. Chang, *Adv. Mater.* **2007**, *19*, 1830.
8	$H_3[(Cu_4Cl)_3\text{-}(BTTri)_8]$	1.58	NA	3.25	A. Demessence, D. M. D'Alessandro, M. L. Foo, J. R. Long, *J. Am. Chem. Soc.* **2009**, *131*, 8784.
9	$(In_3O)(OH)(ADC)_2(NH_2IN)_2 \cdot 2.67H_2O$	2.31	NA	3.21	X. Gu, Z. –H. Lu and Q. Xu, *Chem. Commun.*, **2010**, *46*, 7400.

10	$(In_3O)(OH)(ADC)_2(IN)_2 \cdot 4.67H_2O$	2.08	NA	2.99	X. Gu, Z. –H. Lu and Q. Xu, *Chem. Commun.,* **2010**, *46*, 7400.
11	CPM-6	1.88	4.76	2.90	S.-T. Zheng, J. T. Bu, Y. Li, T. Wu, F. Zuo, P. Feng, X. Bu, *J. Am. Chem. Soc.* **2010**, *132*, 17062.
12	Co-ANIC-1	1.64	4.22	3.48	This work
13	MOF-505	2.48	NA	3.27	B. Chen, N. W. Ockwig, A. R. Millward, D. S. Contreras, O. M. Yaghi, *Angew. Chem. Int. Ed.* **2005**, *44*, 4745.
14	Bio-MOF-11	1.5	6.0	4.0	J. An, S. J. Geib, N. L. Rosi *J. Am. Chem. Soc.* **2010**, 132, 38
15	Zn\DOBDC	1.54	NA	5.5	S. R. Caskey, A. G. Wong-Foy, A. J. Matzger, *J. Am. Chem. Soc.* **2008**, *130*, 10870.
16	$Zn_2(C_2O_4)(C_2N_4H_3)_2.(H_2O)_{0.5}$	1.70	4.30	3.78	R. Vaidhyanathan, S. S. Iremonger, K. W. Dawson, G. K. H. Shimizu, *Chem. Commun.*, **2009**, 5230.
17	ZTF-1	1.6	5.35	3.79	T. Panda, P. Pachfule, Y. Chen, J. Jiang, R. Banerjee *Chem. Commun.*, **2011**, 2011.
18	UMCM-150	2.1	NA	2.8	A. G. Wong-Foy, O. Lebel, and A. J. Matzger *J. Am. Chem. Soc.* 2007, **129**, 15740.
19	$Zn_2(BDC)_2$ (DABCO)	2.0	NA	2.71	H. Chun, D. N. Dybtsev, H. Kim, K. Kim, *Chem. Eur. J.* **2005**, *11*, 3521.
20	IRMOF-3	1.80	NA	2.14	F. Debatin, A. Thomas, A. Kelling, N. Hedin, Z. Bacsik, I. Senkovska, S. Kaskel, M. Junginger, H. Muller, U. Schilde, C. Jager, A. Friedrich, H. J. Holdt *Angew. Chem. Int. Ed.* **2010**, *49*, 1258.
21	CPM-5	1.24	3.62	2.43	S.-T. Zheng, J. T. Bu, Y. Li, T. Wu, F. Zuo, P. Feng, X. Bu, *J. Am. Chem. Soc.* **2010**, *132*, 17062.
22	MOF-177	1.25	NA	1.72	J. L. C. Rowsell, A. R. Millward, K. S. Park, O. M. Yaghi, *J. Am. Chem. Soc.* **2004**, *126*, 5666.

23	MOF-5	1.32	NA	0.92	J. L. C. Rowsell, A. R. Millward, K. S. Park, O. M. Yaghi, *J. Am. Chem. Soc.* **2004**, *126*, 5666.

- ***** The serial numbers given are just for the reference. These are not the actual ranking numbers in all the simultaneous H_2 and CO_2 uptake capacities of MOFs.***

Table S4. Comparison of CO_2 adsorption capacity of MOFs**:

SL. No.**	MOFs	CO_2 uptake mmol/g at 1 bar		Reference
		273K	298K	
1	Mg\DOBDC	NA	8.08	S. R. Caskey, A. G. Wong-Foy, A. J. Matzger, *J. Am. Chem. Soc.* **2008**, *130*, 10870.
2	Co\DOBDC	NA	7.11	S. R. Caskey, A. G. Wong-Foy, A. J. Matzger, *J. Am. Chem. Soc.* **2008**, *130*, 10870.
3	Ni\DOBDC	NA	5.80	S. R. Caskey, A. G. Wong-Foy, A. J. Matzger, *J. Am. Chem. Soc.* **2008**, *130*, 10870.
4	Zn\DOBDC	NA	5.51	S. R. Caskey, A. G. Wong-Foy, A. J. Matzger, *J. Am. Chem. Soc.* **2008**, *130*, 10870.
5	UTSA-20	NA	5.01	Z. Guo, H. Wu, G. Srinivas, Y. Zhou, S. Xiang, Z. Chen, Y. Yang, W. Zhou, M. O'Keeffe, B. Chen, *Angew. Chem. Int. Ed.* **2011**, *50*, 3178.
6	HKUST-1	NA	4.72	Q. M. Wang, D. Shen, M. Bulow, M. L. Lau, S. Deng, F.R. Fitch, N. O. Lemcoff, J. Semanscin, *Microporous and Mesoporous Materials*. **2002**, *55*, 217.
7	Zn + 4,4' bipy + (BTA-TBA)	NA	4.10	O. K. Farha. C. D. Malliakas, M. G. Kanatzidis, J. T. Hupp, *J. Am. Chem. Soc.* **2010**, *132*, 950.
8	Bio-MOF-11	6.0	4.01	J. An, S. J. Geib, N. L. Rosi *J. Am. Chem. Soc.* **2010**, *132*, 38.
9	$[Zn_2(1)(DMF)_2]_n(DMF)_m$ [MOF(4)]	5.80	NA	Y.-S. Bae, O. K. Farha, J. T. Hupp, R. Q. Snurr, *J. Mater. Chem.*, **2009**, *19*, 213.
10	$[Zn_3(OH)(p\text{-CDC})_{2.5}]_n$	NA	4.00	Y. S. Bae, O. K. Farha, A. M. Spokoyny, C. A. Mirkin, J. T. Hupp, R. Q. Snurr, *Chem. Commun.*, **2008**, 4135.
11	Cd-ANIC-1	4.72	3.84	This work

12	ZTF-1	5.35	3.79	T. Panda, P. Pachfule, Y. Chen, J. Jiang, R. Banerjee *Chem. Commun*., **2011**, 2011.
13	$Zn_2(C_2O_4)(C_2N_4H_3)_2.(H_2O)_{0.5}$	4.30	3.78	R. Vaidhyanathan, S. S. Iremonger, K. W. Dawson, G. K. H. Shimizu, *Chem. Commun*., **2009**, 5230.
14	Co-ANIC-1	4.22	3.48	This work
15	CUK-1	NA	3.48	J. W. Yoon, S. H. Jhung, Y. K. Hwang, S. M. Humphrey, P. T. Wood, J. S. Chang, *Adv. Mater.* **2007**, *19*, 1830.
16	YO-MOF	NA	3.39	K. L. Mulfort, O. K. Farha, C. D. Malliakas, M. G. Kanatzidis, J. T. Hupp, *Chem. Eur. J.* **2010**, *16*, 276.
17	SNU-M10	NA	3.30	H. S. Choi, M. P. Suh, *Angew. Chem*. **2009**, *121*, 6997.
18	MOF-505	NA	3.27	B. Chen, N. W. Ockwig, A. R. Millward, D. S. Contreras, O. M. Yaghi, *Angew. Chem. Int. Ed.* **2005**, *44*, 4745.
19	$H_3[(Cu_4Cl)_3\text{-}(BTTri)_8]$	NA	3.25	A. Demessence, D. M. D'Alessandro, M. L. Foo, J. R. Long, *J. Am. Chem. Soc.* **2009**, *131*, 8784.
20	$(In_3O)(OH)(ADC)_2(NH_2IN)_2 \bullet 2.67\ H_2O$	NA	3.21	X. Gu, Z. –H. Lu and Q. Xu, *Chem. Commun.,* **2010**, *46*, 7400.
21	CPM-6	4.76	2.90	S.-T. Zheng, J. T. Bu, Y. Li, T. Wu, F. Zuo, P. Feng, X. Bu, *J. Am. Chem. Soc.* **2010**, *132*, 17062.
22	TMA@ Bio-MOF-1,	4.5	NA	J. An and N. L. Rosi, *J. Am. Chem. Soc.* **2010**, *132*, 5578.
23	TEA@ Bio-MOF-1	4.2	NA	J. An and N. L. Rosi, *J. Am. Chem. Soc.* **2010**, *132*, 5578.
24	TBA@ Bio-MOF-1	3.5	NA	J. An and N. L. Rosi, *J. Am. Chem. Soc.* **2010**, *132*, 5578.
25	UMCM-150	NA	2.80	A. G. Wong-Foy, O. Lebel, A. J. Matzger *J. Am. Chem. Soc.* **2007**, *129*, 15740.
26	$Zn_2(BDC)_2$ (DABCO)	NA	2.71	H. Chun, D. N. Dybtsev, H. Kim, K. Kim, *Chem. Eur. J.* **2005**, *11*, 3521.

27	CPM-5	3.62	2.43	S.-T. Zheng, J. T. Bu, Y. Li, T. Wu, F. Zuo, P. Feng, X. Bu, *J. Am. Chem. Soc.* **2010**, *132*, 17062.
28	ZIF-78	3.348	2.23	R. Banerjee, H. Furukawa, D. Britt, C. Knobler, M. O'Keeffe, O. M. Yaghi, *J. Am. Chem. Soc.* **2009**, *131*, 3875.
29	ZIF-96	NA	2.16	W. Morris, B. Leung, H. Furukawa, O. K. Yaghi, N. He, H. Hayashi, Y. Houndonougbo, M. Asta, B. B. Laird, O. M. Yaghi, *J. Am. Chem. Soc.*, **2010**, *132*, 11006.
30	IRMOF-3	NA	2.14	F. Debatin, A. Thomas, A. Kelling, N. Hedin, Z. Bacsik, I. Senkovska, S. Kaskel, M. Junginger, H. Muller, U. Schilde, C. Jager, A. Friedrich, H. J. Holdt *Angew. Chem. Int. Ed.* **2010**, *49*, 1258
31	$(In_3O)(OH)(ADC)_2(IN)_2 \cdot 4.67\ H_2O$	NA	2.08	X. Gu, Z. –H. Lu and Q. Xu, *Chem. Commun.*, **2010**, *46*, 7400.
32	MOF-177	NA	1.72	J. L. C. Rowsell, A. R. Millward, K. S. Park, O. M. Yaghi, *J. Am. Chem. Soc.* **2004**, *126*, 5666.
33	ZIF-69	3.03	1.69	R. Banerjee, H. Furukawa, D. Britt, C. Knobler, M. O'Keeffe, O. M. Yaghi, *J. Am. Chem. Soc.* **2009**, *131*, 3875.
34	MOF-5	NA	0.92	J. L. C. Rowsell, A. R. Millward, K. S. Park, O. M. Yaghi, *J. Am. Chem. Soc.* **2004**, *126*, 5666.

- ***** The serial numbers given are just for the reference. These are not the actual ranking numbers in allover CO_2 uptake capacities in MOFs.***

Table S5. Comparison of H_2 adsorption capacities in MOFs**:

SL. No.**	Name of MOFs	H_2 uptake wt % at 1bar 77 K	Reference
1	PCN-12	3.05	X. –S. Wang, S. Ma, P. M. Forster, D. Yuan, J. Eckert, J. J. Lopez, B. J. Murphy, J. B. Parise, H. –C. Zhou *Angew. Chem. Int. Ed.* **2008**, *47*, 7263.
2	UTSA-20	2.80	Z. Guo, H. Wu, G. Srinivas, Y. Zhou, S. Xiang, Z. Chen, Y. Yang, W. Zhou, M. O'Keeffe, B. Chen, *Angew. Chem. Int. Ed.* **2011**, *50*, 3178.
3	PCN-14	2.70	S. Ma, D. Sun, J. M. Simmons, C. D. Collier, D. Yuan, H.-C. Zhou, *J. Am. Chem. Soc.*, **2008**, *130*, 1012.
4	NOTT-103	2.56	X. Lin, I. Telepen, A. J. Blake, A. Dailly, C. M. Brown, J. M. Simmons, M. Zoppi, G. S. Walker, K. M. Thomas, T. J. Mays, P. Hubberstey, N. R. Champness, M. Schroder, *J. Am. Chem. Soc.*, **2009**, *131*, 2159.
5	PCN-11	2.55	X. S. Wang, S. Ma, K. Rauch, J. M. Simmons, D. Yuan, X. Wang, T. Yildirim, W. C. Cole, J. J. Lspez, A. de Meijere, H. C. Zhou, *Chem. Mater.,* **2008**, 20, 3145.
6	HKUST-1	2.54	Q. M. Wang, D. Shen, M. Bulow, M. L. Lau, S. Deng, F.R. Fitch, N. O. Lemcoff, J. Semanscin, *Microporous and Mesoporous Materials*. **2002**, *55*, 217.
7	Cu_2(tptc)	2.52	X. Lin, J. H. Jia, X. B. Zhao, K. M. Thomas, A. J. Blake, G. S. Walker, N. R. Champness, P. Hubberstey, M. Schroder, *Angew. Chem., Int. Ed.,* **2006**, *45*, 7358.
8	NOTT-100	2.52	X. Lin, I. Telepen, A. J. Blake, A. Dailly, C. M. Brown, J. M. Simmons, M. Zoppi, G. S. Walker, K. M. Thomas, T. J. Mays, P. Hubberstey, N. R. Champness, M. Schroder, *J. Am. Chem. Soc.*, **2009**, *131*, 2159.
9	NOTT-140	2.50	C.Tan, S. Yang, N. R. Champness, X.Lin, A. J. Blake, W. Lewis, M. Schroder, *Chem. Commun.,* **2011**, 4487.

10	MOF-505	2.48	B. Chen, N. W. Ockwig, A. R. Millward, D. S. Contreras, O. M. Yaghi, *Angew. Chem. Int. Ed.* **2005**, *44*, 4745.
11	NOTT-101	2.46	X. Lin, I. Telepen, A. J. Blake, A. Dailly, C. M. Brown, J. M. Simmons, M. Zoppi, G. S. Walker, K. M. Thomas, T. J. Mays, P. Hubberstey, N. R. Champness, M. Schroder, *J. Am. Chem. Soc.*, **2009**, *131*, 2159.
12	NOTT-105	2.46	X. Lin, I. Telepen, A. J. Blake, A. Dailly, C. M. Brown, J. M. Simmons, M. Zoppi, G. S. Walker, K. M. Thomas, T. J. Mays, P. Hubberstey, N. R. Champness, M. Schroder, *J. Am. Chem. Soc.*, **2009**, *131*, 2159.
13	$Cu_4Cl(btt)_{3/8}$	2.42	M. Dinca, W. S. Han, Y. Liu, A. Dailly, C. M. Brown, J. R. Long, *Angew. Chem., Int. Ed.*, **2007**, *46*, 1419.
14	$Cu_6O(tzi)_3(NO_3)$	2.40	F. Nouar, J. F. Eubank, T. Bousquet, L. Wojtas, M. J. Zaworotko, M. Eddaoudi, *J. Am. Chem. Soc.*, **2008**, *130*, 1833.
15	PCN-12’	2.40	X. –S. Wang, S. Ma, P. M. Forster, D. Yuan, J. Eckert, J. J. Lopez, B. J. Murphy, J. B. Parise, H. –C. Zhou *Angew. Chem. Int. Ed.* **2008**, *47*, 7263.
16	PCN-10	2.34	X. S. Wang, S. Ma, K. Rauch, J. M. Simmons, D. Yuan, X. Wang, T. Yildirim, W. C. Cole, J. J. Lspez, A. de Meijere, H. C. Zhou, *Chem. Mater.,* **2008**, 20, 3145.
17	$(In_3O)(OH)(ADC)_2(NH_2IN)_2 \cdot 2.67H_2O$	2.31	X. Gu, Z. –H. Lu and Q. Xu, *Chem. Commun.*, **2010**, *46*, 7400.
18	NU-100	2.29	O. K. Farha, A. O. Yazaydın, I. Eryazici, C. D. Malliakas, B. G. Hauser, M. G. Kanatzidis, S. T. Nguyen, R. Q. Snurr, J. T. Hupp, *Nature Chem.* **2010**, *2*, 944.
19	NOTT-112	2.30	Y.Yan, X. Lin, S. Yang, A. J. Blake, A. Dailly, N. R. Champness, P. Hubbersteya, M. Schroder, *Chem. Commun*., **2009**, 1025.
20	NOTT-109	2.28	X. Lin, I. Telepen, A. J. Blake, A. Dailly, C. M. Brown, J. M. Simmons, M. Zoppi, G. S. Walker, K. M. Thomas, T. J. Mays, P. Hubberstey, N. R. Champness, M. Schroder, *J. Am. Chem. Soc.*, **2009**, *131*, 2159.

21	PCN-61	2.25	D. Yuan, D. Zhao, D. Sun, Hong-Cai Zhou, *Angew. Chem. Int. Ed.* **2010**, *49*, 5357.
22	Mn-BTT	2.25	M. Dinca, A. Dailly, Y. Liu, C. M. Brown, D. A. Neumann, J. R. Long, *J. Am. Chem. Soc.* **2006**, 128, 16876.
23	Cu_2(qptc)	2.24	X. Lin, J. Jia, X. Zhao, K. M. Thomas, A. J. Blake, G. S. Walker, N. R. Champness, P. Hubberstey, M. Schroder, *Angew.Chem.* **2006**, 118, 7518.
24	NOTT-106	2.24	X. Lin, I. Telepen, A. J. Blake, A. Dailly, C. M. Brown, J. M. Simmons, M. Zoppi, G. S. Walker, K. M. Thomas, T. J. Mays, P. Hubberstey, N. R. Champness, M. Schroder, *J. Am. Chem. Soc.*, **2009**, *131*, 2159.
25	NOTT-107	2.21	X. Lin, I. Telepen, A. J. Blake, A. Dailly, C. M. Brown, J. M. Simmons, M. Zoppi, G. S. Walker, K. M. Thomas, T. J. Mays, P. Hubberstey, N. R. Champness, M. Schroder, *J. Am. Chem. Soc.*, **2009**, *131*, 2159.
26	$[Zn_2(1)(DMF)_2]_n(DMF)_m$ [MOF(4)]	2.20	O. K. Farha, K. L. Mulfort, J. T. Hupp, *Inorg. Chem.*.; **2008**, *47*, 10223.
27	NOTT-102	2.19	X. Lin, I. Telepen, A. J. Blake, A. Dailly, C. M. Brown, J. M. Simmons, M. Zoppi, G. S. Walker, K. M. Thomas, T. J. Mays, P. Hubberstey, N. R. Champness, M. Schroder, *J. Am. Chem. Soc.*, **2009**, *131*, 2159.
28	$[Zn_3(OH)(p\text{-}CDC)_{2.5}(DEF)_4](4)$	2.10	O. K. Farha, A. M. Spokoyny, K. L. Mulfort, M. F. Hawthorne, C. A. Mirkin, J. T. Hupp, *J. Am. Chem. Soc.*, **2007**, *129*, 12680.
29	MOC-2	2.17	D. F. Sava, V.C. Kravtsov, J. Eckert, J. F. Eubank, F. Nouar, M. Eddaoudi, *J. Am. Chem. Soc.*, **2009**, *131*, 10394.
30	UMCM-150	2.10	A. G. Wong-Foy, O. Lebel, A. J. Matzger *J. Am. Chem. Soc.* **2007**, *129*, 15740.
31	Ni\DOBDC	2.10	S. R. Caskey, A. G. Wong-Foy, A. J. Matzger, *J. Am. Chem. Soc.* **2008**, *130*, 10870.

32	$Zn_2(BDC)(TMBDC)(DABCO)$	2.10	H. Chun, D. N. Dybtsev, H. Kim, K. Kim, *Chem. Eur. J.* **2005**, *11*, 3521
33	$Ni_3(BTC)_2(3\text{-}PIC)_6(PD)_3$	2.10	X. B. Zhao, B. Xiao, A. J. Fletcher, K. M. Thomas, D. Bradshaw, M. J. Rosseinsky, *Science* **2004**, *306*, 1012.
34	$(In_3O)(OH)(ADC)_2(IN)_2 \bullet 4.67H_2O$	2.08	X. Gu, Z. –H. Lu and Q. Xu, *Chem. Commun.*, **2010**, *46*, 7400.
35	$Zn_2(BDC)_2$ (DABCO)	2.00	H. Chun, D. N. Dybtsev, H. Kim, K. Kim, *Chem. Eur. J.* **2005**, *11*, 3521.
36	Mg\DOBDC	1.98	S. R. Caskey, A. G. Wong-Foy, A. J. Matzger, *J. Am. Chem. Soc.* **2008**, *130*, 10870.
37	PCN-6	1.90	D. Sun, S. Ma, Y. Ke, D. J. Collins, H. C. Zhou, *J. Am. Chem. Soc.* **2006**, 128, 3896.
38	NOTT-116	1.90	Y. Yan, I. Telepeni, S. Yang, X. Lin, W. Kockelmann, A. Dailly, A. J. Blake, W. Lewis, G. S. Walker, D. R. Allan, S. A. Barnett, N. R. Champness, M. Schroder, *J. Am. Chem. Soc.* **2010**, 132, 4092.
39	CPM-6	1.88	S.-T. Zheng, J. T. Bu, Y. Li, T. Wu, F. Zuo, P. Feng, X. Bu, *J. Am. Chem. Soc.* **2010**, *132*, 17062.
40	PCN-68	1.87	D. Yuan, D. Zhao, D. Sun, Hong-Cai Zhou, *Angew. Chem. Int. Ed.* **2010**, *49*, 5357.
41	Cd-ANIC-1	1.84	This work
42	Co\DOBDC	1.81	S. R. Caskey, A. G. Wong-Foy, A. J. Matzger, *J. Am. Chem. Soc.* **2008**, *130*, 10870.
43	IRMOF-3	1.80	F. Debatin, A. Thomas, A. Kelling, N. Hedin, Z. Bacsik, I. Senkovska, S. Kaskel, M. Junginger, H. Muller, U. Schilde, C. Jager, A. Friedrich, H. J. Holdt *Angew. Chem. Int. Ed.* **2010**, *49*, 1258.
44	PCN-66	1.79	D. Yuan, D. Zhao, D. Sun, Hong-Cai Zhou, *Angew. Chem. Int. Ed.* **2010**, *49*, 5357.

45	$Zn_2(C_2O_4)(C_2N_4H_3)_2.(H_2O)_{0.5}$	1.70	R. Vaidhyanathan, S. S. Iremonger, K. W. Dawson, G. K. H. Shimizu, *Chem. Commun.*, **2009**, 5230.
46	Co-ANIC-1	1.64	This work
47	$[Co_4(OH)_2(p\text{-}CDC)_3 DMF_2]_n$ (2)	1.61	O. K. Farha, A. M. Spokoyny, K. L. Mulfort, S. Galli, J. T. Hupp, C. A. Mirkin, *small* **2009**, *5*, 1727.
48	ZTF-1	1.60	T. Panda, P. Pachfule, Y. Chen, J. Jiang, R. Banerjee *Chem. Commun.*, **2011**, 2011.
49	CUK-1	1.60	J. W. Yoon, S. H. Jhung, Y. K. Hwang, S. M. Humphrey, P. T. Wood, J. S. Chang, *Adv. Mater.* **2007**, *19*, 1830.
50	$H_3[(Cu_4Cl)_3\text{-}(BTTri)_8]$	1.58	A. Demessence, D. M. D'Alessandro, M. L. Foo, J. R. Long, *J. Am. Chem. Soc.* **2009**, *131*, 8784.
51	Zn\DOBDC	1.54	S. R. Caskey, A. G. Wong-Foy, A. J. Matzger, *J. Am. Chem. Soc.* **2008**, *130*, 10870.
52	Bio-MOF-11	1.50	J. An, S. J. Geib, N. L. Rosi *J. Am. Chem. Soc.* **2010**, *132*, 38
53	ZIF-11	1.37	K. S. Park, Z. Ni, A. P. Cote, J. Y. Choi, R. D. Huang, F. J. Uribe-Romo, H. K. Chae, M. O'Keeffe and O. M. Yaghi, *Proc. Natl. Acad.Sci. U. S. A.*, **2006**, *103*, 10186.
54	MOF-5	1.32	J. L. C. Rowsell, A. R. Millward, K. S. Park, O. M. Yaghi, *J. Am. Chem. Soc.* **2004**, *126*, 5666.
55	ZIF-8	1.30	K. S. Park, Z. Ni, A. P. Cote, J. Y. Choi, R. D. Huang, F. J. Uribe-Romo, H. K. Chae, M. O'Keeffe and O. M. Yaghi, *Proc. Natl. Acad.Sci. U. S. A.*, **2006**, *103*, 10186.
56	MOF-177	1.25	J. L. C. Rowsell, A. R. Millward, K. S. Park, O. M. Yaghi, *J. Am. Chem. Soc.* **2004**, *126*, 5666.
57	CPM-5	1.24	S.-T. Zheng, J. T. Bu, Y. Li, T. Wu, F. Zuo, P. Feng, X. Bu, *J. Am. Chem. Soc.* **2010**, *132*, 17062.

- ***** The serial numbers given are just for the reference. These are not the actual ranking numbers in allover H_2 uptake capacities in MOFs.***

Section S5. Single crystal structures of MOFs:

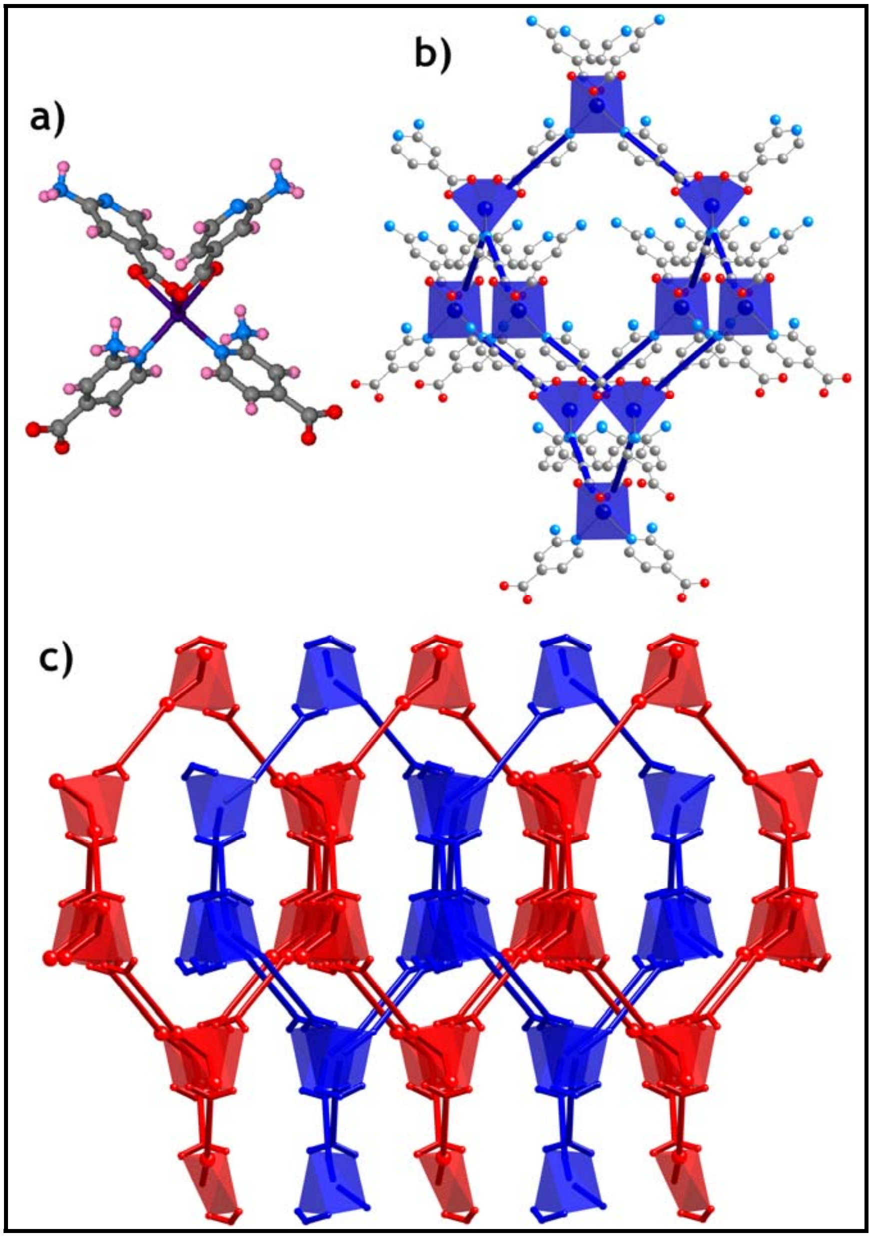

Figure S10. Crystal structure of Cd-ANIC-1 and Co-ANIC-1. (a) Octahedral SBU in Cd-ANIC-1 and Co-ANIC-1 where each octahedral SBU is connected to the two μ_2-OCO carboxylate groups and two nitrogen atoms from the ANIC ligand. (b) A single adamantanoid cage of Cd-ANIC-1 and Co-ANIC-1, where blue lines show the formation of adamantanoid cage. (c) Interpenetrated adamantanoid cages in Cd-ANIC-1 and Co-ANIC-1.

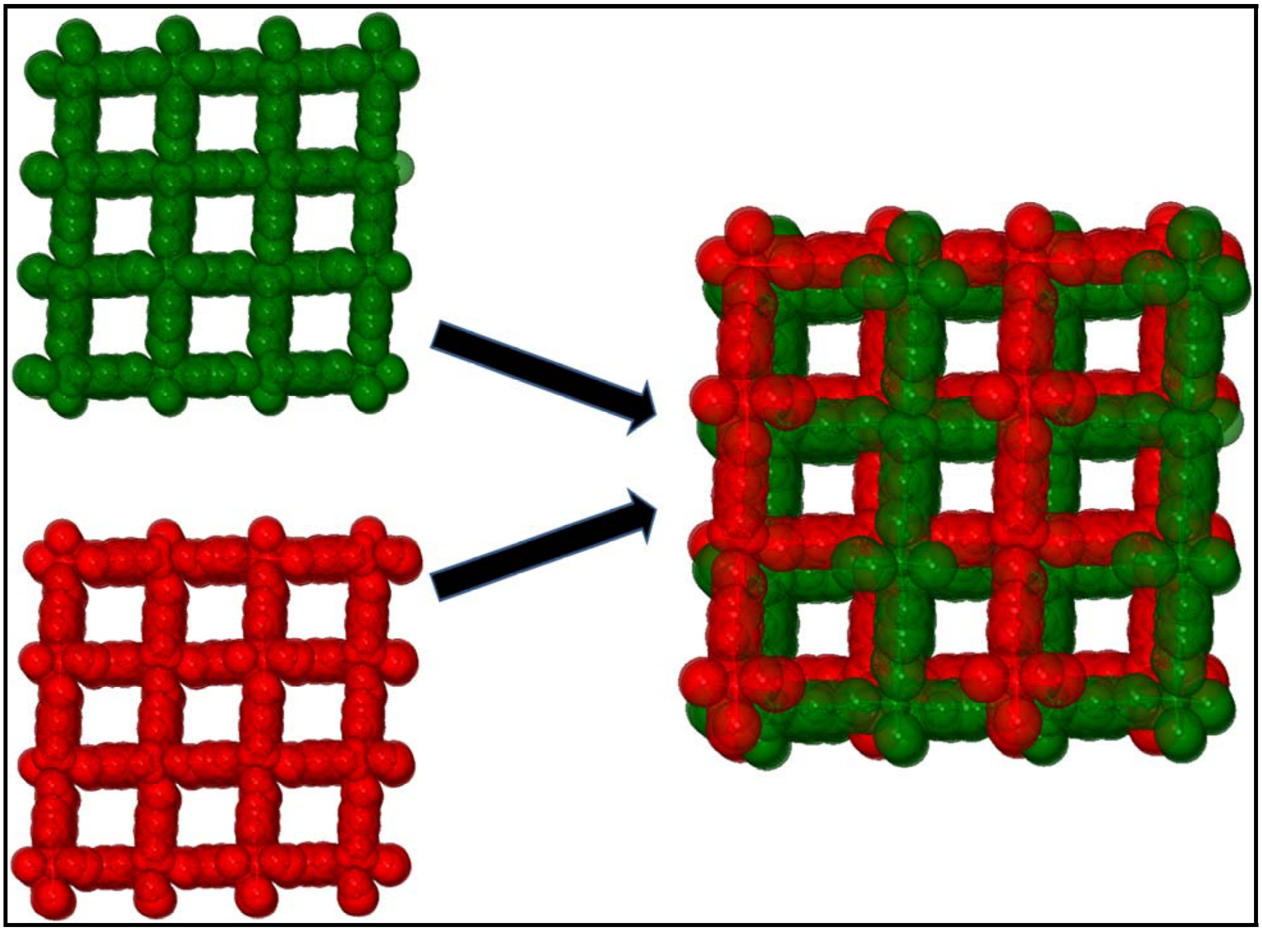

Figure S11. Formation of the interpenetrated framework showing pores available for gas adsorption in Cd-ANIC-1 and Co-ANIC-1, where separate green and red colored layers are interweaving to form the interpenetrated framework through *a* axis.

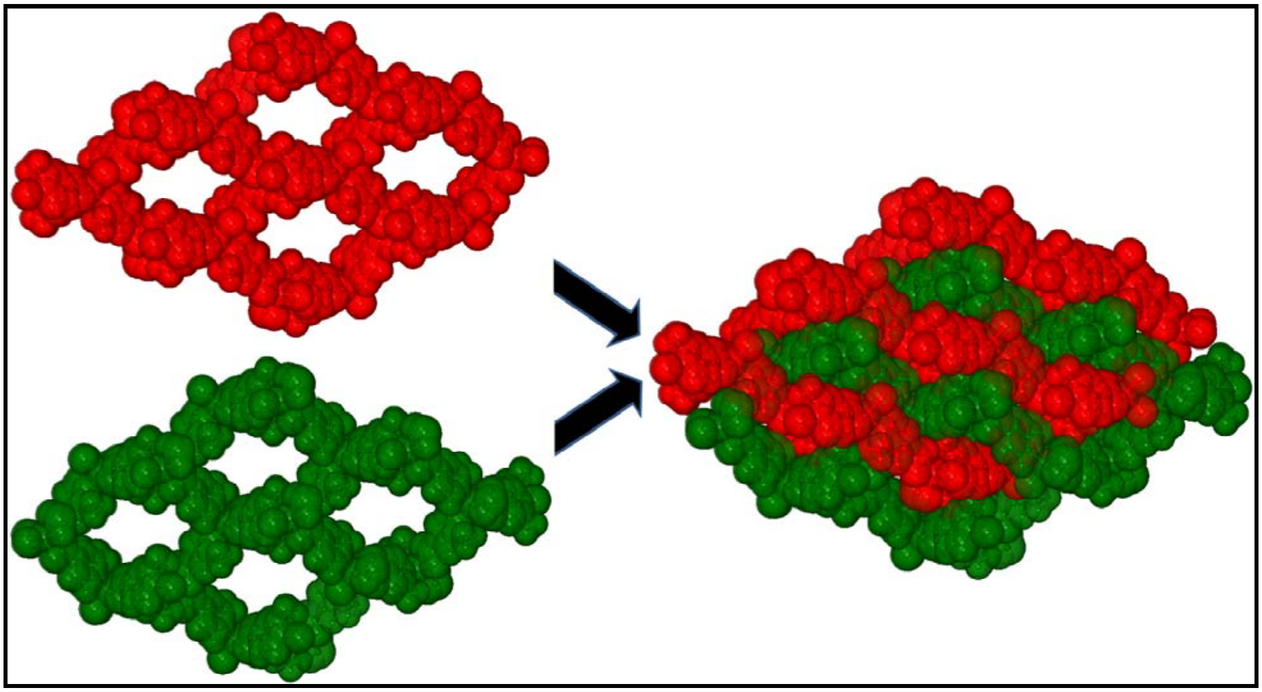

Figure S12. Formation of the interpenetrated framework in Cd-ANIC-1 and Co-ANIC-1, where separate green and red colored layers are interweaving to form the interpenetrated framework through *b* axis.

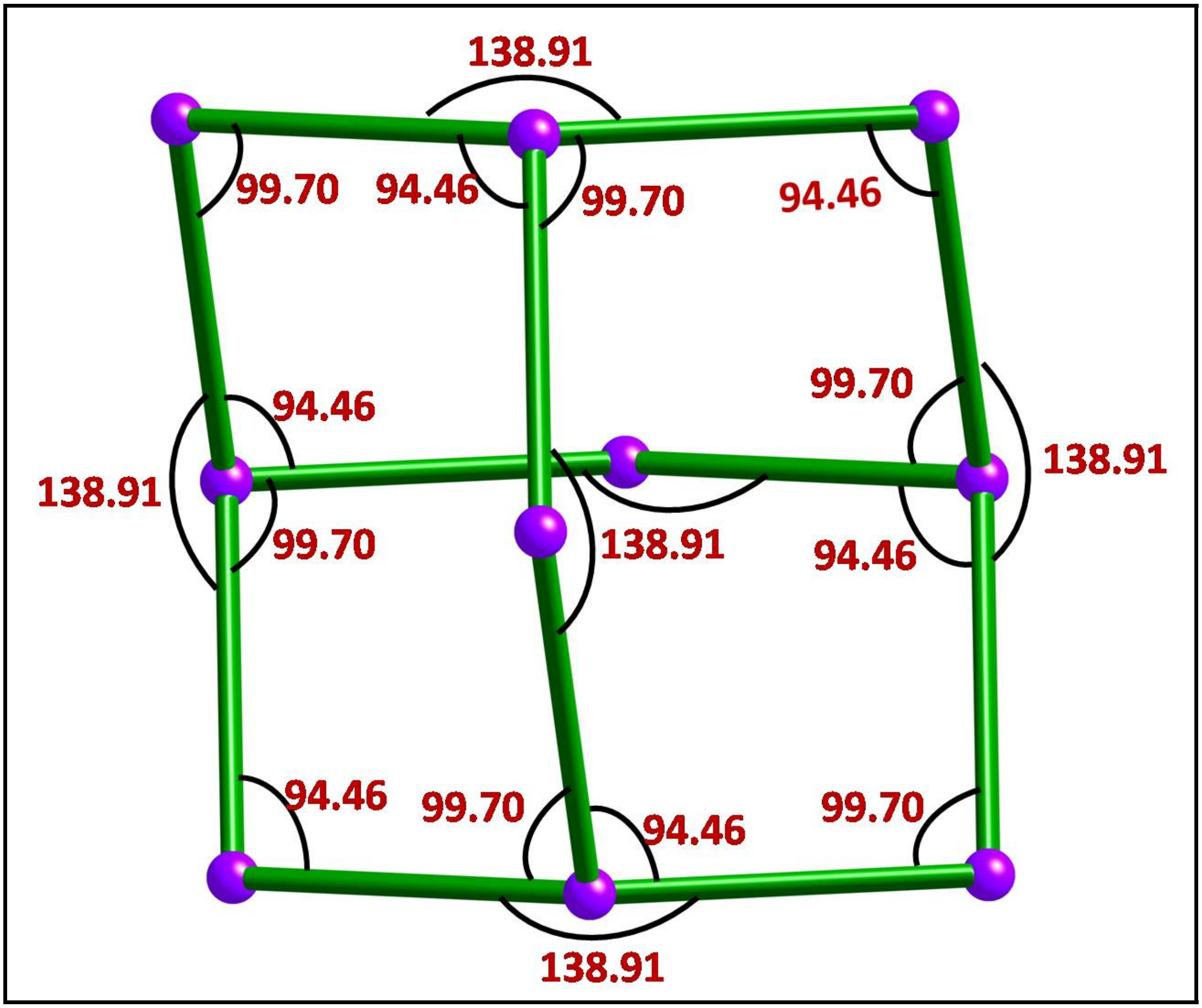

Figure S13. Three types (out of 18) of L–M–L angles are present in the adamantanoid cage in Cd-ANIC-1; each 6 are 138.91º, 99.70º and 94.46º. The angles between the each corners of hexagonal circuit (99.70º and 94.46º) are less than the angles at middle of hexagonal circuit (138.91º).

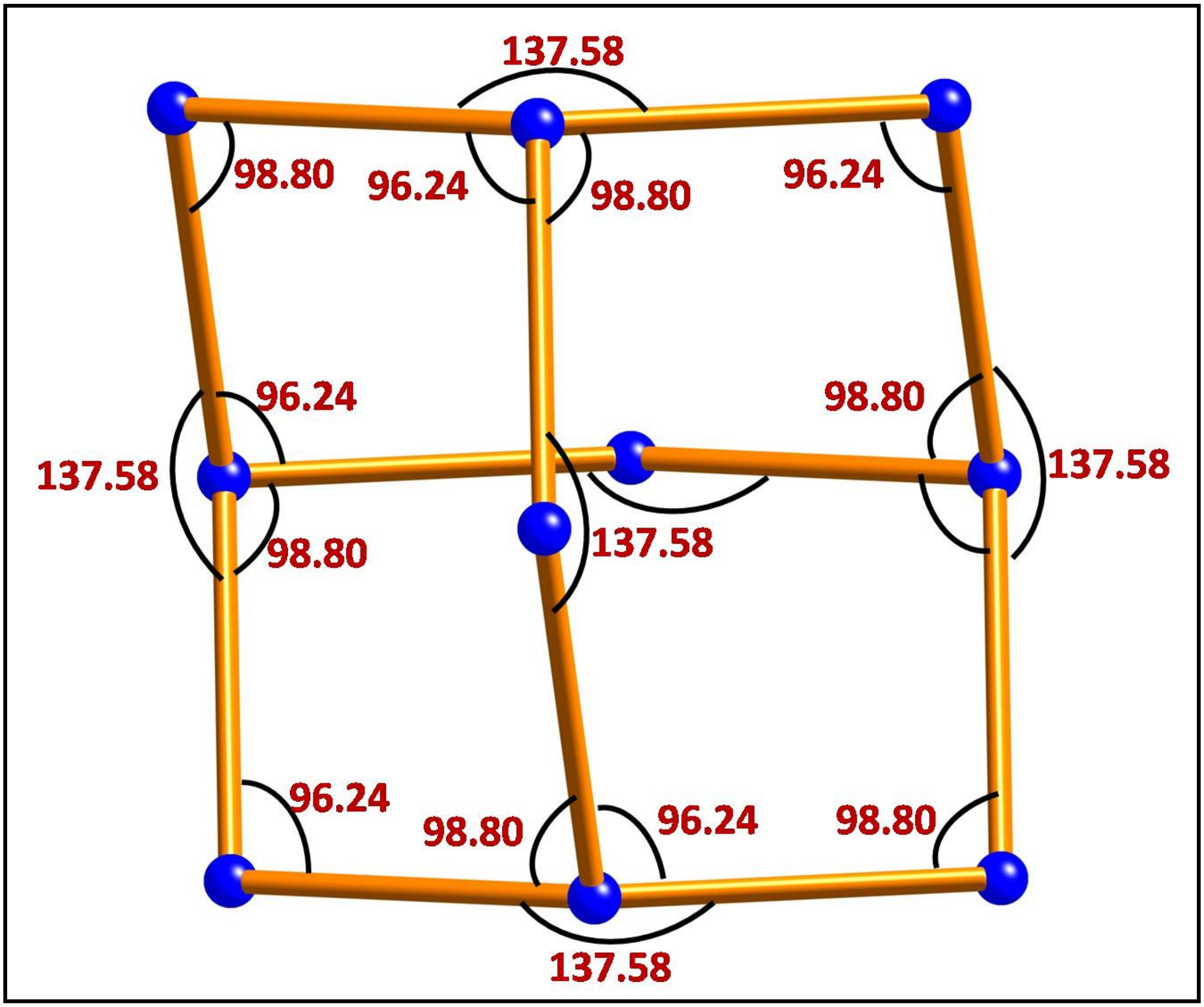

Figure S14. Three types (out of 18) of L–M–L angles are present in the adamantanoid cage in Co-ANIC-1; each 6 are 137.58º, 98.80º and 96.24º. The angles between the each corners of hexagonal circuit (98.80º and 96.24º) are less than the angles at middle of hexagonal circuit (137.58º).

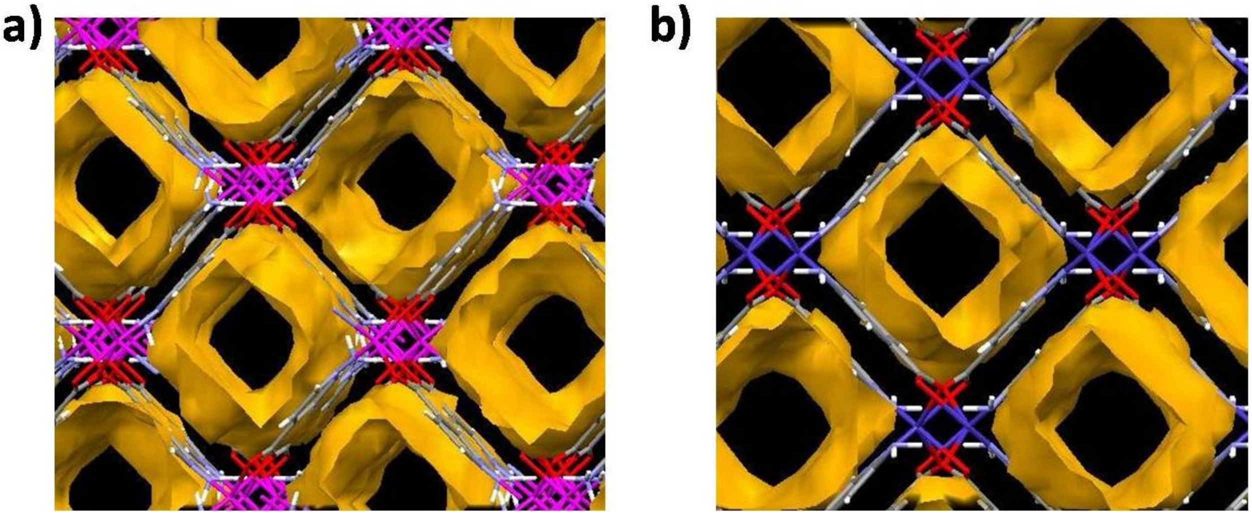

Figure 15. (a) Empty voids calculated using Mercury from the Cambridge Structural Database, by selecting a probe molecule with a radius of ca. 1.2 Å centered at the central part of the pore. 38.2 % solvent accessible volume available in Cd-ANIC-1 due to higher metal–metal (Cd–Cd = 9.167 Å) distance and lower degree of interpenetration. (b) Empty voids calculated using Mercury from the Cambridge Structural Database, by selecting a probe molecule with a radius of ca. 1.2 Å centered at the central part of the pore. 36.3 % solvent accessible volume available in Co-ANIC-1 due to lower metal–metal (Co–Co = 8.858 Å) distance and higher degree of interpenetration.

Section S6. Computational Studies for MOFs:

Simulation Models and Methods

Grand-canonical Monte Carlo (GCMC) simulations were carried for the adsorption of H_2 at 77 K and CO_2 at 298 K in Cd-ANIC-1 and Co-ANIC-1. H_2 was represented as a two-site rigid molecule with H–H bond length of 0.74 Å. The Lennard-Jones parameters of H-H interaction were $\sigma = 2.59$ Å and $\varepsilon = 12.5$ K.[1] CO_2 was represented as a three-site rigid molecule and its intrinsic quadrupole moment was described by a partial-charge model. The partial charges on C and O atoms were $q_C = 0.576e$ and $q_O = -0.288e$ ($e = 1.6022 \times 10^{-19}$ is the elementary charge). The C–O bond length was 1.18 Å and the bond angle O–C–O was 180°. The LJ parameters for CO_2 were $\sigma_C = 2.789$ Å, $\varepsilon_C = 29.66$ K, $\sigma_O = 3.011$ Å, $\varepsilon_O = 82.96$ K.[2]

The experimentally determined crystal structures were used in simulations. The porosities of Cd-ANIC-1 and Co-ANIC-1 were estimated to be approximately 0.516 and 0.488 using Materials Studio[3] with a Connolly probe radius equal to zero. The atomic charges of the framework atoms were calculated from periodic density functional theory (DFT) using the primitive cells of Cd-ANIC-1 and Co-ANIC-1. The DFT calculations used the Becke exchange plus Lee-Yang-Parr correlation functional and all-electron core potentials. The double-ξ numerical polarization (DNP) basis set was adopted. The Mulliken population analysis was used to estimate the atomic charges as listed in Table S6. The dispersion interactions of the framework atoms in Cd-ANIC-1 and Co-ANIC-1 were modeled using the parameters based on the DREIDING force field.[4] However, the DREIDING force field parameters are not available for Cd and Co atoms; thus the parameters from the Universal force field were adopted.[5] With these LJ parameters, the predicted isotherms were found not to agree well with experimental data. As a simple alternative, the parameters of carbon atoms were adjusted. Table S7 lists the set of LJ parameters used in this study. The Lorentz-Berthelot combining rules were used to calculate the cross LJ interaction parameters.

Table S6. Atomic charges in Cd-ANIC-1 and Co-ANIC-1. The atomic types are labeled in Figure S16.

	(a) Cd-ANIC-1						
Atom type	C1	C2	C3	C4	C5	C6	Cd
Charge	0.314	0.030	-0.059	0.525	-0.048	0.213	0.953
Atom type	H1	H2	H3	H4	N1	N2	O
Charge	0.079	0.255	0.136	0.029	-0.476	-0.565	-0.581
	(b) Co-ANIC-1						
Atom type	C1	C2	C3	C4	C5	C6	Cd
Charge	0.271	-0.028	-0.051	0.553	-0.041	0.189	0.711
Atom type	H1	H2	H3	H4	N1	N2	O
Charge	0.074	0.175	0.144	0.046	-0.700	-0.246	-0.574

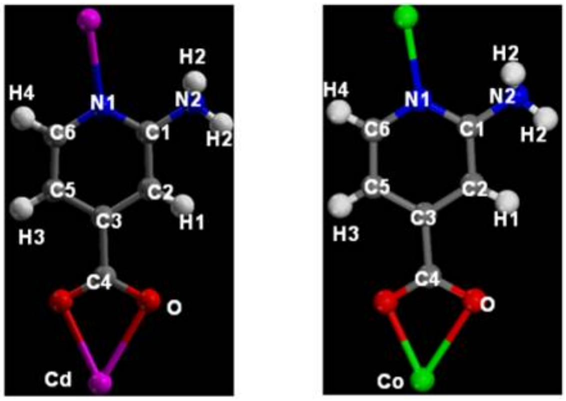

Figure S16. Atomic types in Cd-ANIC-1 and Co ANIC-1.

Table S7. LJ Potential Parameters for the framework atoms involved in Cd-ANIC-1 and Co-ANIC-1.

Atom type	**Cd**	**Co**	**C(in Cd-ANIC-1)**	**C(in Co-ANIC-1)**	**O**	**N**	**H**
σ (Å)	2.537	2.559	3.473	3.473	3.033	3.263	2.846
ε/k_B (K)	114.631	7.039	40.813	32.813	48.115	38.914	7.642

In the GCMC simulations, the frameworks were treated as rigid and the adsorbent-adsorbate interactions were pre-tabulated. The LJ interactions were evaluated using a spherical cutoff of 11.5 Å with the long-range corrections added. For the Coulombic interactions, the Ewald sum with a tin-foil boundary condition was used. The real/reciprocal space partition parameter and the cutoff for reciprocal lattice vectors were chosen to be 0.2 Å^{-1} and 8, respectively, to ensure the convergence of the Ewald sum. Five types of trial moves were conducted for gas molecules, namely, displacement, rotation, partial regrowth at a neighboring position, complete regrowth at a new position, and swap with the reservoir. The number of trial moves in the simulation was 2× 10^7 with the first 10^7 moves for equilibration and the subsequent 10^7 moves for production.

Results and Discussion

Figure S17 shows the adsorption isotherms for H_2 at 77 K and CO_2 at 298 K in Cd-ANIC-1 and Co-ANIC-1. The simulated results of H_2 agree fairly well with the experimental data in both structures. However, the simulated results of CO_2 are overestimated at low pressures and underestimated at high pressures. These deviations could be attributed to a number of possible factors. First, the framework structures used in simulations are perfect crystals without any defects; however, experimental samples usually contain impurities. Second, activation of experimental samples may not be complete and solvent is not fully evacuated. Finally, the force field used may be inaccurate to describe the interactions. For both H_2 and CO_2, the extent of adsorption in Cd-ANIC-1 is greater than in Co-ANIC-1 because the former has a larger porosity.

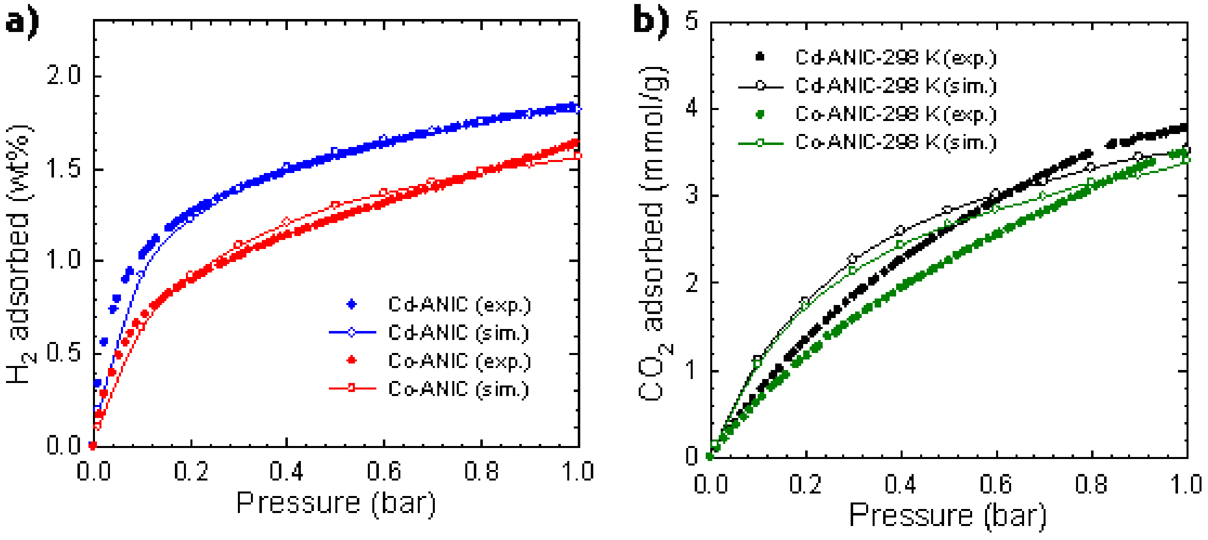

Figure S17. Adsorption isotherms in Cd-ANIC-1 and Co-ANIC-1 (a) H_2 at 77 K (b) CO_2 at 298 K. The open symbols are from simulation and the filled symbols are from experiment.

Figure S18 shows the density contours of H_2 adsorption at 77 K and 1 kPa in Cd-ANIC-1 and Cd-ANIC-1. The contours are viewed from the (100) plane and generated by accumulating 100 equilibrium configurations. It is observed that H_2 molecules are primarily adsorbed in the pore centers in both Cd-ANIC-1 and Cd-ANIC-1. CO_2 adsorption shows similar density contours.

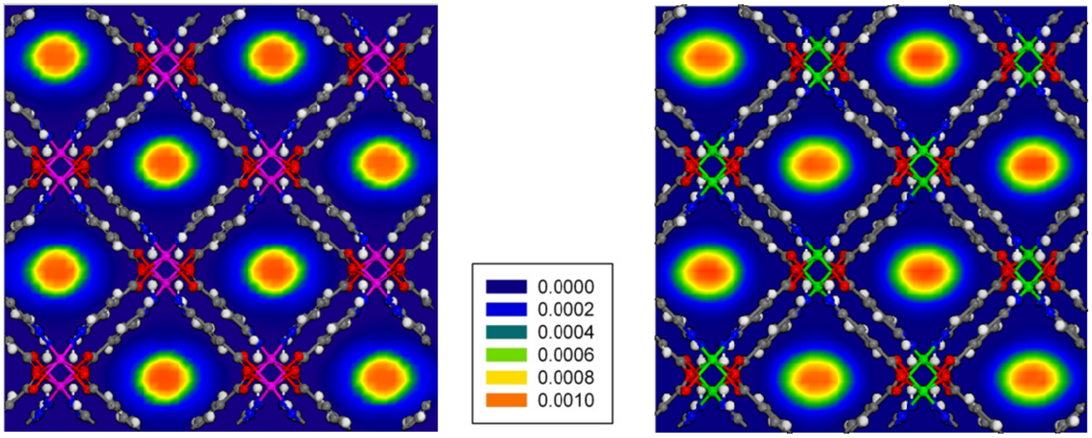

Figure S18. Density contours of H_2 adsorption at 1 kPa in (a) Cd-ANIC-1 and (b) Co-ANIC-1.

To better understand the nature of adsorption sites, Figure S19a shows the radial distribution functions $g(r)$ between CO_2 and the framework atoms (C2, Cd, O, N2) in Cd-ANIC-1. The $g(r)$ was calculated by

$$g_{ij}(r) = \frac{\Delta N_{ij}\, V}{4\pi r^2 \Delta r\, N_i N_j}$$

where r is the distance between species i and j, ΔN_{ij} is the number of species j around i within a shell from r to $r + \Delta r$, V is the volume, N_i and N_j are the numbers of species i and j. It is observed CO_2 is the closest to C2 atom and the $g(r)$ of CO_2-C2 has the highest peak. This reveals that phenyl ring has the strongest affinity with CO_2 because of the framework interpenetration. CO_2

is closer to N2 atom than to Cd and O atoms, implying –NH_2 group plays a more important role than Cd and O atoms for CO_2 adsorption. Figure S19b schematically shows the distances between a single CO_2 molecule and the framework atoms. Figure S20a shows the radial distribution functions and distances between CO_2 and the framework atoms (C2, Co, O, N2) in Co-ANIC-1. Similar to Figure S20b, CO_2 is the closest to C2 atom, followed by N2 atom, and finally O and Co atoms. Again, this suggests CO_2 is preferentially adsorbed near phenyl ring and then –NH_2 group.

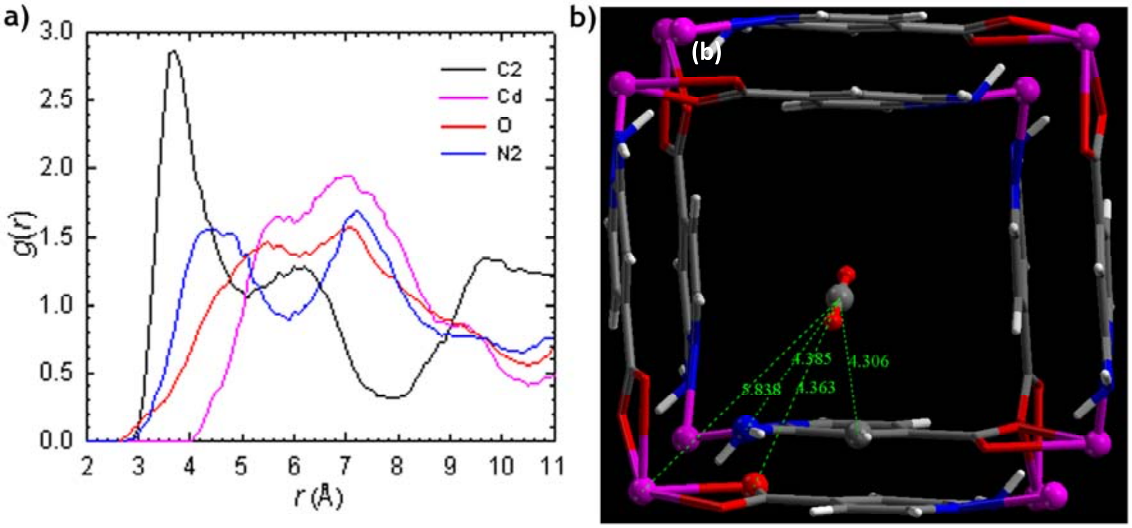

Figure S19. (a) Radial distribution functions and (b) distances between CO_2 and framework atoms (C2, Cd, O, N2) in Cd-ANIC-1.

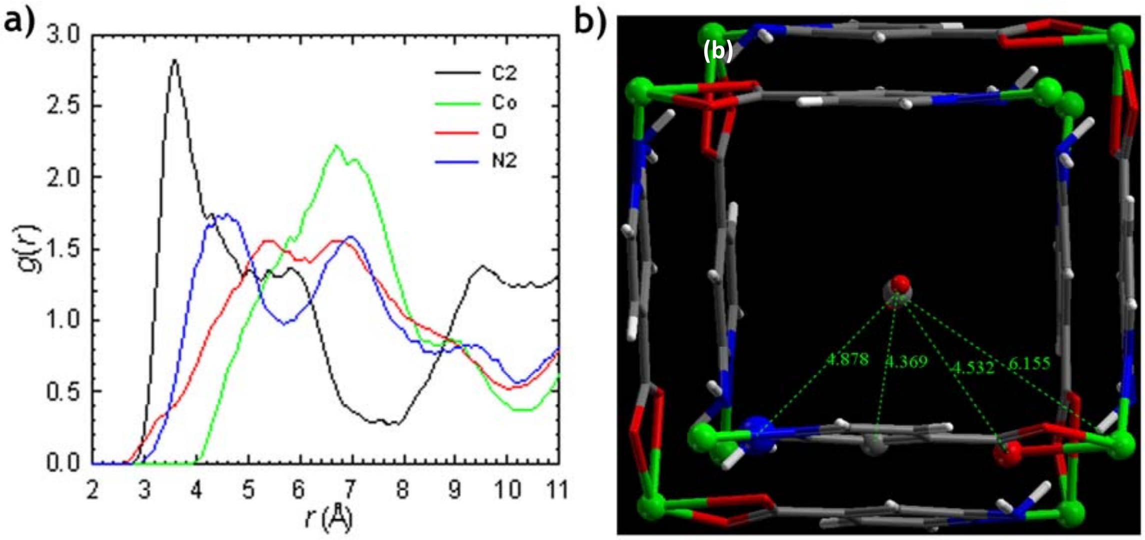

Figure S20. (a) Radial distribution functions and (b) distances between CO_2 and framework atoms (C2, Co, O, N2) in Co-ANIC-1.

Table S8: Cd-ANIC-1: CO_2 Adsorption Isotherms-

Cd-ANIC-1: CO_2 Adsorption Isotherms							
EXPERIMENTAL ADSORPTION ISOTHERMS				**SIMULATED ADSORPTION ISOTHERMS**			
273 K		**298 K**		**273 K**		**298 K**	
Pressure (bar)	CO_2 adsorbed (mmol/g)	Pressure (bar)	CO_2 adsorbed (mmol/g)	Pressure (bar)	CO_2 adsorbed (mmol/g)	Pressure (bar)	CO_2 adsorbed (mmol/g)
4.04E-04	0.0031	4.72E-04	9.33E-04	0.01	0.366	0.01	0.136
0.01208	0.18454	0.01384	0.10763	0.1	2.29751	0.1	1.1109
0.0235	0.35378	0.02765	0.21535	0.2	3.12073	0.2	1.78159
0.03939	0.57927	0.04256	0.32634	0.3	3.52825	0.3	2.26348
0.05075	0.73303	0.05289	0.40327	0.4	3.81143	0.4	2.59295
0.06431	0.9072	0.06519	0.49324	0.5	4.00379	0.5	2.82911
0.07714	1.06212	0.07746	0.58058	0.6	4.17396	0.6	3.01537
0.09361	1.24902	0.08981	0.66597	0.7	4.26657	0.7	3.16192
0.10544	1.37626	0.1072	0.78	0.8	4.35234	0.8	3.31906
0.11951	1.5188	0.11728	0.84183	0.9	4.45363	0.9	3.44187
0.13375	1.65476	0.13242	0.93723	1	4.54525	1	3.52118
0.14781	1.78159	0.14438	1.01322				
0.1632	1.91153	0.16386	1.12893				
0.17755	2.02627	0.17568	1.19962				
0.1923	2.13715	0.18909	1.27727				
0.20711	2.24286	0.20049	1.34101				
0.22081	2.33576	0.21446	1.41456				
0.22808	2.38614	0.22695	1.47548				
0.24008	2.46161	0.24438	1.56449				
0.25463	2.54915	0.25524	1.62265				
0.27248	2.64956	0.26715	1.68442				
0.28708	2.72868	0.28604	1.77311				
0.30138	2.80242	0.30235	1.84763				
0.30836	2.8402	0.3154	1.90704				
0.32294	2.91004	0.32269	1.93428				
0.33678	2.9747	0.33998	2.00654				
0.3512	3.03931	0.34812	2.04532				
0.3649	3.09783	0.36679	2.1203				
0.37718	3.14992	0.38384	2.18786				
0.38922	3.19923	0.38971	2.21611				
0.40767	3.26885	0.40053	2.25872				
0.41728	3.30707	0.41714	2.31714				

0.42989	3.35346	0.42908	2.3559				
0.44624	3.41048	0.44214	2.40623				
0.46461	3.47148	0.45584	2.45846				
0.47959	3.5213	0.46885	2.50711				
0.48598	3.54524	0.48558	2.56407				
0.50051	3.59056	0.49657	2.60312				
0.51412	3.63232	0.50838	2.63569				
0.52563	3.66716	0.52784	2.69721				
0.53806	3.70357	0.53776	2.73322				
0.5494	3.73712	0.54983	2.7735				
0.56502	3.77975	0.56166	2.81419				
0.5783	3.81646	0.57979	2.87118				
0.59701	3.86436	0.5903	2.90883				
0.60454	3.88755	0.6043	2.95232				
0.62206	3.93137	0.61792	2.99265				
0.63657	3.96864	0.63031	3.02055				
0.64931	4.00195	0.64833	3.06895				
0.6613	4.03348	0.65933	3.10333				
0.67255	4.06282	0.67141	3.1413				
0.69158	4.10615	0.68589	3.18497				
0.69858	4.12717	0.69799	3.22116				
0.71453	4.1637	0.70912	3.25522				
0.7278	4.19448	0.72277	3.29087				
0.7386	4.22059	0.74134	3.33681				
0.75692	4.25942	0.75241	3.36901				
0.77133	4.29141	0.76384	3.39655				
0.78392	4.3187	0.78371	3.44165				
0.79316	4.32644	0.79482	3.47037				
0.81353	4.3565	0.83971	3.5639				
0.82193	4.37816	0.84281	3.57132				
0.83997	4.41714	0.84843	3.59448				
0.84627	4.43919	0.8682	3.63576				
0.8638	4.47713	0.87848	3.64462				
0.8774	4.50793	0.89002	3.66293				
0.89418	4.5414	0.90424	3.69555				
0.90196	4.55963	0.92004	3.71225				
0.9195	4.58704	0.92988	3.73084				
0.93093	4.60203	0.94579	3.74813				
0.9416	4.62552	0.95901	3.76906				
0.95985	4.66072	0.97195	3.79231				

0.97067	4.67894	0.98323	3.82109				
0.98579	4.70597	0.995	3.8332				
0.99569	4.7256						

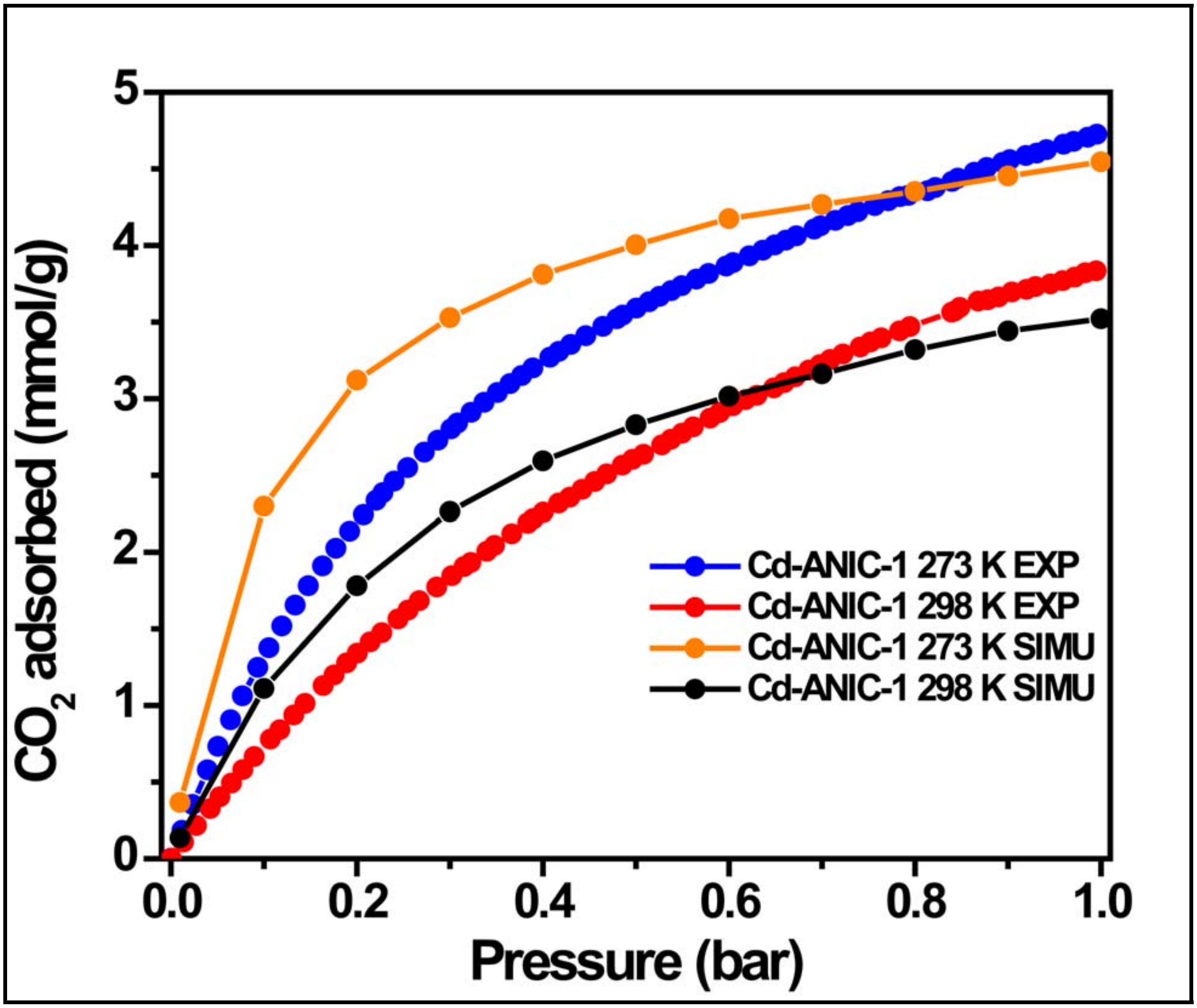

Figure S21. Experimental and simulated CO$_2$ adsorption isotherms for Cd-ANIC-1 at 273 K (blue and brown circles) and 298 K (red and black circles).

Table S9: Co-ANIC-1: CO_2 Adsorption Isotherms-

Co-ANIC-1: CO_2 Adsorption Isotherms							
EXPERIMENTAL ADSORPTION ISOTHERMS				**SIMULATED ADSORPTION ISOTHERMS**			
273 K		**298 K**		**273 K**		**298 K**	
Pressure (bar)	CO_2 adsorbed (mmol/g)	Pressure (bar)	CO_2 adsorbed (mmol/g)	Pressure (bar)	CO_2 adsorbed (mmol/g)	Pressure (bar)	CO_2 adsorbed (mmol/g)
6.14E-04	2.02E-03	5.48E-04	0.00258	0.01	0.372	0.01	0.138
0.0195	0.11374	0.016	0.10839	0.1	2.15	0.1	1.07
0.0422	0.25148	0.0303	0.2079	0.2	2.96	0.2	1.72
0.06	0.36237	0.0433	0.29492	0.3	3.36	0.3	2.14
0.077	0.46102	0.0554	0.37231	0.4	3.68	0.4	2.44
0.102	0.61348	0.0711	0.4602	0.5	3.84	0.5	2.67
0.119	0.70726	0.0841	0.53922	0.6	4	0.6	2.84
0.142	0.8393	0.0963	0.61914	0.7	4.12	0.7	2.99
0.162	0.94507	0.109	0.68994	0.8	4.24	0.8	3.15
0.186	1.0757	0.128	0.78822	0.9	4.34	0.9	3.24
0.199	1.15068	0.136	0.83643	1	4.39	1	3.39
0.225	1.29624	0.148	0.88199				
0.24	1.37915	0.159	0.94564				
0.265	1.5097	0.18	1.05953				
0.286	1.62834	0.189	1.10813				
0.3	1.70239	0.204	1.16088				
0.322	1.80998	0.22	1.238				
0.344	1.91494	0.228	1.27492				
0.377	2.06855	0.247	1.38091				
0.389	2.12884	0.264	1.42397				
0.402	2.19225	0.271	1.45822				
0.426	2.28935	0.282	1.50865				
0.462	2.45115	0.299	1.57359				
0.474	2.50682	0.309	1.60475				
0.488	2.56934	0.328	1.68191				
0.503	2.63357	0.335	1.70581				
0.529	2.7149	0.354	1.76305				
0.544	2.77718	0.369	1.82165				
0.568	2.86097	0.384	1.874				
0.59	2.94025	0.4	1.93759				
0.622	3.05818	0.412	1.97511				
0.635	3.11085	0.424	2.01378				

0.648	3.16452	0.437	2.04977				
0.681	3.27839	0.446	2.07926				
0.691	3.32054	0.464	2.12752				
0.706	3.3742	0.472	2.15115				
0.729	3.43698	0.484	2.1951				
0.751	3.49942	0.501	2.24662				
0.774	3.5644	0.519	2.31191				
0.789	3.61353	0.533	2.35617				
0.828	3.72261	0.545	2.38221				
0.839	3.75973	0.561	2.42908				
0.852	3.80361	0.567	2.45041				
0.889	3.90791	0.585	2.49851				
0.9	3.94587	0.6	2.53933				
0.913	3.98715	0.608	2.56371				
0.934	4.0434	0.627	2.61365				
0.966	4.12865	0.633	2.6349				
0.987	4.19184	0.651	2.67556				
0.994	4.20411	0.658	2.69783				
		0.675	2.74205				
		0.693	2.7903				
		0.708	2.82938				
		0.723	2.86021				
		0.731	2.88828				
		0.743	2.92262				
		0.775	2.99782				
		0.784	3.02539				
		0.792	3.04041				
		0.81	3.09536				
		0.826	3.13297				
		0.839	3.16698				
		0.855	3.21129				
		0.867	3.2344				
		0.881	3.27027				
		0.893	3.3005				
		0.904	3.31728				
		0.917	3.35975				
		0.93	3.38182				
		0.971	3.45823				
		0.984	3.47873				
		0.9954	3.48734				

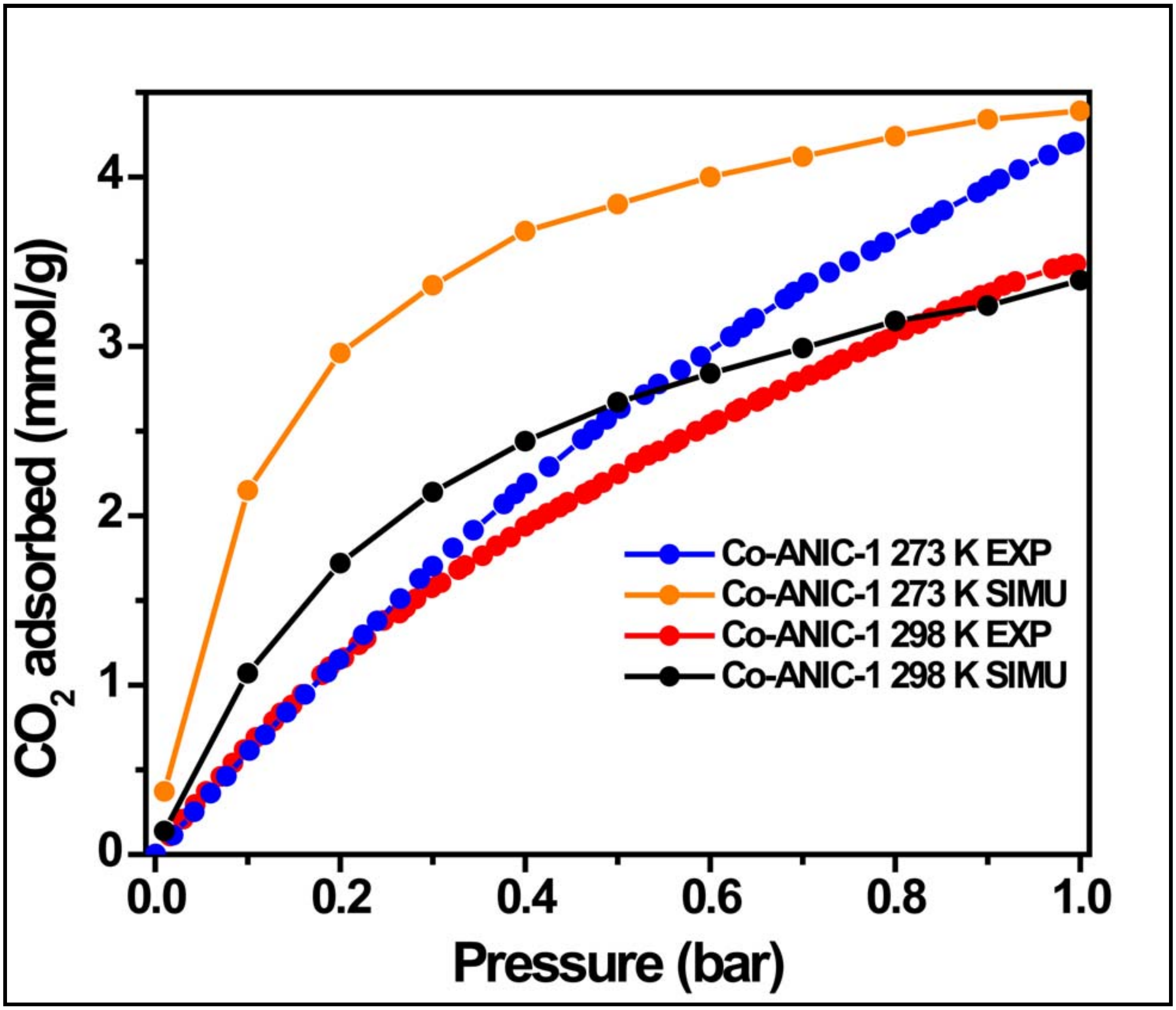

Figure S22. Experimental and simulated CO_2 adsorption isotherms for Co-ANIC-1 at 273 K (blue and brown circles) and 298 K (red and black circles).

Table S10: Cd-ANIC-1 and Co-ANIC-1: H_2 Adsorption Isotherms-

EXPERIMENTAL ADSORPTION ISOTHERMS				**SIMULATED ADSORPTION ISOTHERMS**			
Cd-ANIC-1		**Co-ANIC-1**		**Cd-ANIC-1**		**Co-ANIC-1**	
Pressure (bar)	H_2 adsorbed (mmol/g)	Pressure (bar)	H_2 adsorbed (mmol/g)	Pressure (bar)	H_2 adsorbed (mmol/g)	Pressure (bar)	H_2 adsorbed (mmol/g)
1.79E-04	2.07E-03	4.13E-04	0.00105	0.01	0.19451	0.01	0.10644
0.01023	0.34041	0.0125	0.17177	0.1	0.92773	0.1	0.64308
0.02367	0.56142	0.0225	0.28122	0.2	1.22848	0.2	0.92178
0.04234	0.73893	0.0387	0.39628	0.3	1.39389	0.3	1.08884
0.04885	0.79721	0.0526	0.49345	0.4	1.50593	0.4	1.20802
0.06773	0.90128	0.0672	0.55937	0.5	1.59097	0.5	1.30269
0.07605	0.94233	0.0775	0.60985	0.6	1.65379	0.6	1.36881
0.10118	1.03026	0.0899	0.66038	0.7	1.70273	0.7	1.42819
0.10918	1.0592	0.108	0.71251	0.8	1.75355	0.8	1.48543
0.11953	1.08957	0.127	0.75594	0.9	1.79342	0.9	1.52342
0.12973	1.11723	0.136	0.7749	1	1.81742	1	1.56436
0.15689	1.17521	0.145	0.79926				
0.16706	1.19685	0.158	0.82475				
0.17863	1.21917	0.173	0.85164				
0.20331	1.26143	0.205	0.89732				
0.21602	1.28101	0.215	0.91833				
0.22618	1.29729	0.229	0.93636				
0.23764	1.31333	0.24	0.95523				
0.28756	1.37417	0.29	1.01285				
0.2954	1.38369	0.303	1.03026				
0.30697	1.39671	0.311	1.04192				
0.32256	1.41247	0.321	1.0577				
0.33762	1.42676	0.341	1.07328				
0.34989	1.43967	0.355	1.09045				
0.36022	1.44936	0.365	1.10126				
0.37482	1.46375	0.375	1.11502				
0.38869	1.47561	0.388	1.12668				
0.40662	1.49045	0.403	1.14066				
0.42307	1.50416	0.423	1.15437				
0.43739	1.51468	0.433	1.16749				
0.44645	1.52369	0.443	1.17575				
0.46417	1.53584	0.461	1.19292				
0.47487	1.54545	0.47	1.20163				

0.48825	1.55458	0.484	1.21611				
0.50519	1.5664	0.497	1.22608				
0.51854	1.57637	0.512	1.23548				
0.52812	1.58299	0.523	1.25082				
0.54063	1.59355	0.536	1.25942				
0.55382	1.60222	0.55	1.27401				
0.56623	1.61036	0.567	1.28472				
0.58036	1.62054	0.587	1.29457				
0.59458	1.62798	0.601	1.31084				
0.60572	1.63559	0.607	1.31689				
0.61897	1.64274	0.618	1.32768				
0.63161	1.65292	0.634	1.34045				
0.64402	1.65988	0.651	1.35097				
0.65864	1.6701	0.663	1.3618				
0.67077	1.67726	0.672	1.3771				
0.68341	1.68362	0.685	1.38524				
0.69828	1.69394	0.707	1.39434				
0.71179	1.70002	0.722	1.4067				
0.73232	1.70981	0.734	1.42025				
0.7432	1.71717	0.747	1.4321				
0.75311	1.72569	0.761	1.43951				
0.77246	1.73438	0.774	1.45566				
0.78605	1.74333	0.788	1.46433				
0.79328	1.74629	0.797	1.46928				
0.81125	1.75406	0.811	1.48706				
0.82615	1.76343	0.825	1.49255				
0.8427	1.76986	0.839	1.49879				
0.85138	1.77343	0.855	1.51574				
0.8596	1.77947	0.868	1.52539				
0.87804	1.78593	0.88	1.53085				
0.89105	1.79108	0.893	1.54947				
0.9053	1.79462	0.902	1.55436				
0.92228	1.80312	0.919	1.56097				
0.93752	1.8068	0.933	1.57821				
0.94547	1.81269	0.945	1.58511				
0.96159	1.82251	0.956	1.59637				
0.97077	1.82555	0.971	1.614				
0.98943	1.83098	0.982	1.619				
0.995	1.8354	0.989	1.62609				
--	--	0.995	1.63523				

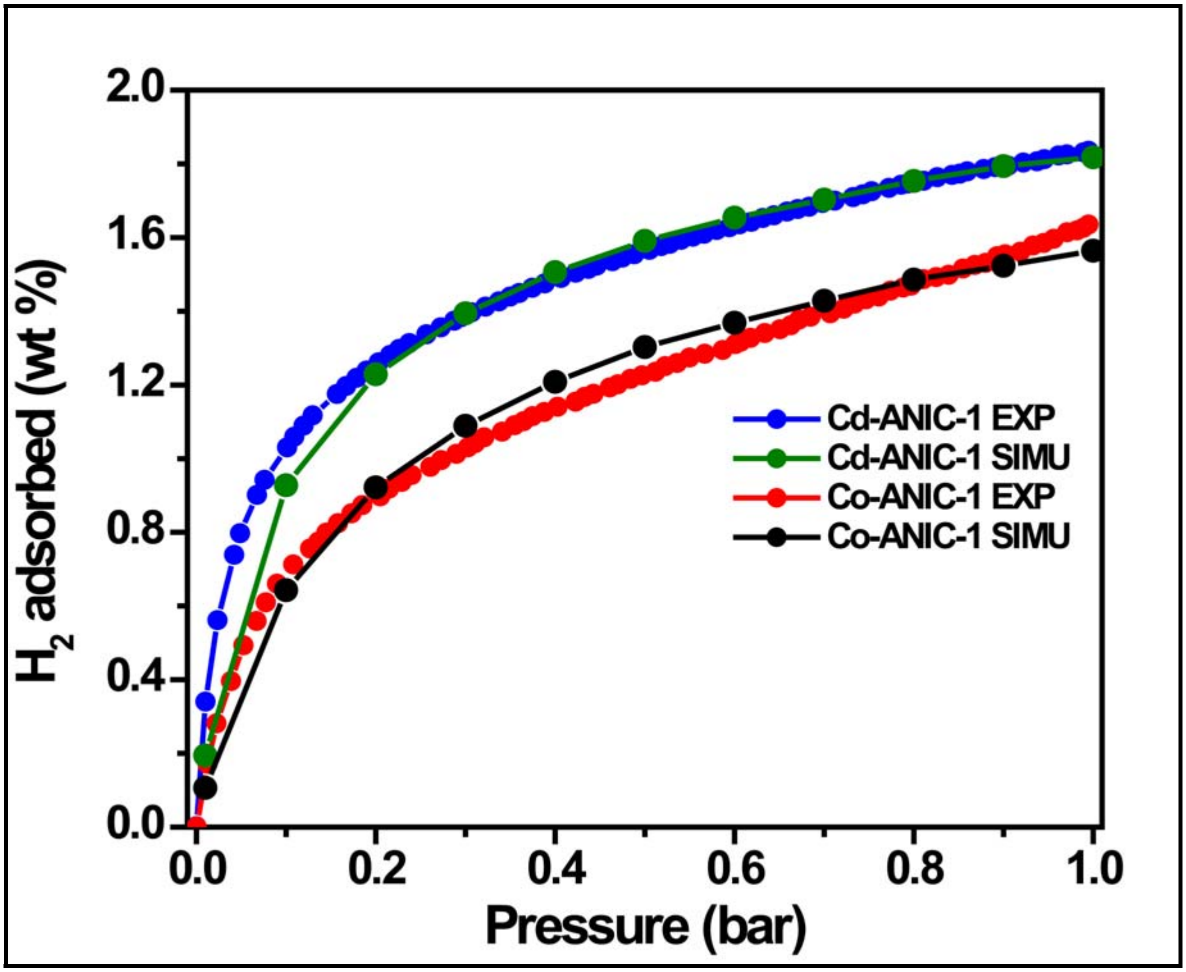

Figure S23. Experimental and simulated H_2 adsorption isotherms for Cd-ANIC-1 (blue and green circles) and Co-ANIC-1 (red and black circles).

References:

(1) Cracknell, R. F., *Phys. Chem. Chem. Phys.* 2001, *3*, 2091.

(2) Hirotani, A.; Mizukami, K.; Miura, R.; Takaba, H.; Miya, T.; Fahmi, A.; Stirling, A.; Kubo, M.; Miyamoto, A., *Appl. Surf. Sci.* 1997, *120*, 81.

(3) Materials Studio, v.4.4, Accelrys: San Diego, 2007.

(4) Mayo, S. L.; Olafson, B. D.; Goddard, W. A., *J. Phys. Chem.* 1990, *94*, 8897.

(5) Rappe, A. K.; Casewit, C. J.; Colwell, K. S.; Goddard, W. A.; Skiff, W. M., *J. Am. Chem. Soc.* 1992, *114*, 10024.